CERN-ACC-2020-0028

October 2020
stephane.fartoukh@cern.ch

Combined ramp and telescopic squeeze

S. Fartoukh, G. Azzopardi, R. Bruce, X. Buffat, J. Coello De Portugal, N. Fuster-Martinez, G. Iadarola, N. Karastathis, S. Kostoglou, E.H. Maclean, L. Malina, A. Mereghetti, D. Mirarchi, T. Persson, M. Pojer, A. Poyet, B. Salvachua, M. Schaumann, M. Solfaroli, G. Sterbini, R. Tomas, D. Valuch, A. Wegscheider, J. Wenninger

Keywords: LHC Run 3, ATS scheme, combined ramp and tele-squeeze

Summary

This paper highlights the outcome of the 2018 round ATS MD program, which aimed at demonstrating the feasibility of a combined ramp and telescopic squeeze as a potential key ingredient to operate the machine in Run 3, with much brighter and more energetic beams with respect to Run 2. The machine configuration which was used is first described in terms of hypercycle, optics transitions, and dedicated beam gymnastics. The various commissioning steps which were needed to obtain the green light for an intensity ramp up are described, in particular the optics measurements and corrections, the triplet aperture measurements, and the collimation-related activities. The main results are illustrated in terms of octupole threshold minimization, beam lifetime in the ramp with the machine filled with several hundred of nominal bunches or 8b4e bunch trains, and long-range beam-beam mitigation with lattice octupoles. A dedicated instability study on possible variants for the adjust beam process is also reported.

1 Introduction

The Achromatic Telescopic Squeezing (ATS) scheme [1] constitutes the baseline optics scheme for the HL-LHC. It was routinely used in operation in 2017 and 2018 in order to further reduce β^*, but still with a rather modest telescopic index of 1.6 reached at the end of the telescopic squeeze from $\beta^* = 40$ cm down to 25 cm (40/25=1.6). This index of 1.6 can indeed be directly compared to sensibly larger values targeted for the HL-LHC, typically ranging from 4 to 8 for round and flat optics, respectively. Actually, the telescopic index not only quantifies the additional β^* squeezing factor offered by the ATS techniques, but it also corresponds to the relative increase of the peak β functions induced in the four arcs adjacent to the two high luminosity insertions ATLAS and CMS. As a result, another interesting by-product of the ATS scheme lies in the fact that it boosts the efficiency of the lattice octupoles (MO), either for increasing the level of Landau damping which

is requested at higher impedance and/or higher beam brightness, or for mitigating the long-range beam-beam (BBLR) interactions, or for both. The gain in MO efficiency is however rather modest at low telescopic indexes (1-1.5), but then rises quite rapidly for higher indexes (going asymptotically with the square of the telescopic index).
The aim of the present MD campaign was to commission a new possible template for the LHC hypercycle, in particular with a "combined ramp and double squeeze" (CRDS) with the tele-squeeze fully deployed in the ramp prior to the completion of the pre-squeeze optics sequence, and to study the properties of this machine configuration from the perspective of the above-mentioned beam dynamics aspects. The merit of this program was therefore to converge towards a possible solution for the Run 3 optics which would be compatible with the full LIU beam intensity (as far as impedance and BBLR effects are concerned), while completing the validation of the ATS scheme for the HL-LHC (at large telescopic index). The ultimate objective of the program, which was successfully reached, was to use this new machine configuration to inject, ramp and collide several hundreds of bunches packed into BCMS [2] and 8b4e trains [3], in order to exclude as well any un-expected effects such as a possible degradation of the electron cloud impact onto the beam, with the peak beta-functions reaching up to 500-600 m in the arcs at the end of the CRDS.
The breakdown structure of the special LHC hypercycle which was used is given in Section 2, with the different beam processes (BP) involved, described in terms of optics, various gymnastics and settings (tune, octupole, ADT, collimator, etc.). An overview of the various MD activities and results is summarized in Section 3, with emphasizes on optics measurements and corrections, octupole threshold in the ramp, beam lifetime in the new ramp, BBLR mitigation with octupoles, and management of possible coherent instabilities in ADJUST when the MO polarity is set to negative.

2 Hypercycle and main settings

2.1 Optics and hypercycle overview

In order to build up the CRDS, a new set of LHC round optics [4] was prepared in an appropriate ordering, as described hereafter.

- The 2017/2018 injection optics ($\beta^* = 11$ m) was re-used.
- The 2017/2018 pre-squeeze sequence was re-used, started earlier in the energy ramp (at about 1 TeV), and stopped earlier at $\beta^* = 2$ m (reached at ~ 2.7 TeV) . It was then immediately followed by a telescopic squeeze (i.e. at constant matching quadrupole settings in IR1 and IR5) in order to deploy a telescopic index of $2.0/0.65 \sim 3.1$, that is to reach a β^* of 65 cm at the end of the ramp. The timing, energy and optics structures of the CRDS are given in Tab. 1.
- The pre-squeeze sequence was then restarted at flat-top energy, keeping constant the telescopic index of above (i.e. at constant quadrupole settings in IR8, IR2, IR4 and IR6), and further reducing the pre-squeezed β^* from 2.0 m down to 77.0 cm. At the end of this process, β^* took therefore the value of $77 \times 0.65/2.0 = 25.025$ cm at IP1 and IP5. This beam process is detailed in Tab. 2.

Matched Point	Time [s]	Parabolic fraction [%]	Optics name in LSA	β^* [cm] at IP1 and 5	Tele-index	Energy [GeV]
1	0	0.1	R2017a_A11mC11mA10mL10m	1100.0	1.000	450
2	15	0.05	R2017a_A11mC11mA10mL10m	1100.0	1.000	452
3	30	0.05	R2017a_A11mC11mA10mL10m	1100.0	1.000	459
4	45	0.05	R2017a_A11mC11mA10mL10m	1100.0	1.000	470
5	60	0.05	R2017a_A11mC11mA10mL10m	1100.0	1.000	485
6	90	0.05	R2017a_A11mC11mA10mL10m	1100.0	1.000	531
7	120	0.05	R2017a_A11mC11mA10mL10m	1100.0	1.000	594
8	160	0.05	R2017a_A11mC11mA10mL10m	1100.0	1.000	705
9	241	0.05	R2017a_A11mC11mA10mL10m	1100.0	1.000	1013
10	293	0.13	R2017a_A970C970A10mL970	970.0	1.000	1277
11	317	0.10	R2017a_A920C920A10mL920	920.0	1.000	1416
12	337	0.15	R2017a_A850C850A10mL850	850.0	1.000	1532
13	361	0.13	R2017a_A740C740A10mL740	740.0	1.000	1671
14	385	0.10	R2017a_A630C630A10mL630	630.0	1.000	1810
15	413	0.10	R2017a_A530C530A10mL530	530.0	1.000	1972
16	437	0.11	R2017a_A440C440A10mL440	440.0	1.000	2111
17	461	0.12	R2017a_A360C360A10mL360	360.0	1.000	2250
18	493	0.15	R2017a_A310C310A10mL300	310.0	1.000	2435
19	525	0.15	R2017a_A230C230A10mL300	230.0	1.000	2620
20	545	0.15	R2017a_A200C200A10mL300	200.0	1.000	2736
21	649	0.15	R2018aT200_A182C182A10mL300	182.5	1.096	3339
22	749	0.20	R2018aT200_A155C155A10mL300	155.0	1.290	3918
23	825	0.15	R2018aT200_A122C122A10mL300	122.5	1.633	4358
24	925	0.16	R2018aT200_A95C95A10mL300	95.0	2.105	4937
25	1025	0.20	R2018aT200_A77C77A10mL300	77.5	2.581	5516
26	1169	0.10	R2018aT200_A65C65A10mL300	65.0	3.077	6350
27	1210	0.05	R2018aT200_A65C65A10mL300	65.0	3.077	6500

Table 1: Timing and energy structure, and optics characteristics of the combined ramp and double squeeze (LSA beam process `RAMP_PELP-SQUEEZE-ATS-65cm_HighTele_V1`). The half-crossing angles in IR1 and IR5 are linearly reduced from 170 μrad down to 120 μrad while the other IP knob functions are nominal. In practice, the quadrupole settings corresponding to two consecutive optics (matched points) are connected with Parabolic-Linear-Parabolic (PLP) functions, with the additional constraint of zeroing at the matched points the current slope dI/dt of each circuit involved. This "rounding in/out" procedure takes some fraction of the overall time, reported above as "parabolic fraction".

Matched Point	Time [s]	Parabolic fraction [%]	Optics name in LSA	β^* [cm] at IP1 and 5	Tele-index	Energy [GeV]
1	0	0.00	R2018aT200_A65C65A10mL300	65.000	3.077	6500
2	32	0.30	R2018aT172_A56C56A10mL300	55.900	3.077	6500
3	65	0.30	R2018aT145_A47C47A10mL300	47.450	3.077	6500
4	102	0.32	R2018aT123_A40C40A10mL300	40.300	3.077	6500
5	138	0.28	R2018aT105_A34C34A10mL300	34.450	3.077	6500
6	177	0.26	R2018aT92_A30C30A10mL300	29.900	3.077	6500
7	213	0.28	R2018aT83_A27C27A10mL300	26.975	3.077	6500
8	247	0.31	R2018aT77_A25C25A10mL300	25.025	3.077	6500

Table 2: Timing table for the squeeze at flat-top energy (LSA beam process `SQUEEZE-6.5TeV-ATS-65cm-25cm_HighTele_V1`).

While the full optics sequence of above was probed with pilot beams in MD1, higher intensity tests were continued in MD2 (with set-up beams), MD3 (with up to 733 nominal bunches packed into BCMS trains) and MD4 (with about 800 intense bunches packed into 8b4e trains) by colliding immediately at the end of the ramp (EoR) with $\beta^* = 65$ cm at IP1 and IP5, and a half-crossing angle in the range of 90-120 μrad (with 120 μrad the default EoR value, i.e. $10.2\,\sigma$ for $\gamma\epsilon = 2.5\,\mu$m). The ramp was played at constant (nominal) tune with a fractional part set to .275/.295. As of MD2, the tunes were set to the collision tunes (.31/.32) immediately at the end of the ramp (LSA beam process `QCHANGE-6.5TeV-HighTele-2018_V1`), and the two beams put in collision using the beam process `PHYSICS-6.5TeV-HighTele-2018_V1` played at constant tune (with no IP shift at IP2 and IP5).

2.2 Collimation

The CRDS was played with (nearly) nominal collimator settings in IR3, IR6 and IR7. The modifications with respect to the 2018 operational functions were indeed kept at the minimum needed in order to minimise the risk for human errors. On the other hand, new TCT and TCL4 functions in IR1 and IR5 (N_σ and center) were needed since the value of β^* reached at the end of the CRDS and used in collision (65 cm) was substantially different. The normalized settings and the machine aperture at flat-top energy are summarized in Tab. 3, using a reference emittance of 3.5 μm.
New energy and β^* interlock thresholds were also prepared for the TCTs. For the TCSPs, only the former were necessary, whereas the β^* interlock thresholds were relaxed, corresponding to the

Family	settings [σ]
IR1/IR5 Aperture	14.5
IR1/IR5 TCTs	11
IR2/IR8 TCTs	37/15
IR6 TCSP/TCDQ	7.5

Table 3: Collimator settings updated for MD3270 (for a reference emittance of 3.5 μm).

TCSP parking limit.
To be noted that the TCSP and TCDQ gaps were slightly open with respect to the nominal settings for Beam 1 towards the end of the ramp, by about 200 μm which was still well within the BETS limits (linear trim starting at 825 s, i.e. at the tele-index of 1.6 of the nominal 25 cm optics, see Tab. 1). This trim was needed to "compensate" for the increase of the horizontal β-function for Beam 1 at the TCDQ during the telescopic squeeze, ensuring the same normalised gap of 7.5 σ for both beams at the end of the ramp. This trim was however not deployed in MD4, since one of the TCDQ BPMs had a drifting value hitting the BETS limits[1]. Indeed, the first fill of MD4, i.e. fill 7338, was dumped by this issue (which also enabled to discover the problem and fix it for nominal operation right after the technical stop).
The aforementioned settings were made operational starting from MD2, when nominal bunches were injected in the machine. For the MD slot with only pilot bunches (MD1), dedicated coarse settings were prepared (see the MD MPP procedure in [5]).
In addition to the preparation and LSA implementation of the necessary collimator functions, collimation activities were mainly focused on the TCT alignment and overall validation of the collimation system. The alignment necessary to prepare the TCT centre functions was carried out in MD2, and the machine validated using a few fills with set–up beams (see Section 3.3). The machine was then re-validated twice for the intensity ramp up with BCMS and 8b4e bunch trains, in MD3 and MD4, respectively (see Sections 3.4 and 3.5).
For future reference, Appendix A reports the TCT centre functions deployed during the MD, and Appendix B shows a collection of reference loss maps.
It is worth reminding the importance of the horizontal phase advance between the extraction kickers (MKD) in IR6 and the TCTs of IR1 and IR5. In principle this phase should be maintained within a tolerance band corresponding to $n\pi \pm 30^\circ$ in order to maximize the β^* reach by squeezing down to $1-1.5\,\sigma$ the retraction between IR6 collimators and the TCTs in IR1 and IR5 [6]. For this specific ATS hypercycle, this was strictly speaking not the case at the end of the ramp, but only after the tune jump from the injection tune (0.275/0.295) to the collision tune (0.31/0.32), leading to an increase of the MKD-TCT5 horizontal phase of both beams by $0.035 \times 360 \sim 13^\circ$ (half of it for the MKD-TCT1 phases), and bringing these phases back inside the tolerance band (or at the limit for the TCT of Beam 2 in IR5). This subtlety was however a non-issue for the MD, due to the still relatively large EoR β^* (compared to 30-40 cm), enabling a substantial TCDQ-TCT retraction of $3.5\,\sigma$ (see Tab. 3).

2.3 Octupoles and chromaticities

New octupole ramp functions were prepared for both polarities, with currents much reduced with respect to the nominal settings towards the end of the ramp, where ± 200 A was found much more than sufficient at high telescopic index for single bunch operation at $1.1 - 1.2 \times 10^{11}$ p/b. For the negative polarity, this current was further pushed down to -350 A and -510 A in multi-bunch operation with BCMS ($1.2\,10^{11}$ p/b) and 8b4e ($1.6\,10^{11}$ p/b) bunch trains, tested in MD3 and MD4, respectively. The MO driven amplitude detuning is indeed boosted with the deployment

[1]The drifting of the readout was a very slow one, developing throughout the year.

of the telescope, with the following scaling laws as a function of the tele-index r_{Tele}:

$$\begin{cases} \dfrac{\partial Q_x}{\partial J_x} = \dfrac{\partial Q_y}{\partial J_y} \propto \dfrac{1}{4}\left[\left(r_{\mathrm{Tele}} + \dfrac{1}{r_{\mathrm{Tele}}}\right)^2\right] \\ \dfrac{\partial Q_x}{\partial J_y} = \dfrac{\partial Q_y}{\partial J_x} \propto \dfrac{1}{2}\left[1 + \dfrac{1}{4}\left(r_{\mathrm{Tele}} + \dfrac{1}{r_{\mathrm{Tele}}}\right)^2\right]. \end{cases} \tag{1}$$

While the direct term is relevant to quantify the relative gain in MO efficiency at negative polarity, the beam stability is mainly sensitive to the crossed term for the positive MO polarity.
The full cycle was adjusted with a chromaticity of 10 units by default (trimmed up to 15 in MD4 with 8b4e beams), using the chromaticity tele-knobs (i.e. acting on the sextupole circuits of sectors 23, 34, 67, and 78).

2.4 ADT

New ADT settings were also implemented in order to cope with the new ramp timing structure, and also with the substantial optics changes in IR4 driven by the telescopic squeeze in the ramp itself. Additional modifications to the ADT settings (sensitivity re-tuned for $1.7\,10^{11}$ p/b) were needed in MD4 with the more intense 8b4e beam.

3 Highlights

3.1 MD program overview

The MD program was distributed over the four LHC MD blocks of 2018. The OP mechanics together with optics measurements and corrections successfully took place in MD1 (see Section 3.2). The validation of this new machine configuration was conducted in MD2 with loss maps and asynchronous beam dump tests, together with the implementation of new ramp functions for the Landau octupoles in order to confirm the substantially reduced octupole thresholds at high telescopic index (see Section 3.3). The intensity ramp up took place in MD3 (after a fast re-validation), where up to 733 nominal bunches were injected, ramped and put into collision (see Section 3.4), with a very decent beam lifetime measured in the ramp and a rather small crossing angle reachable in collision ($95\,\mu$rad, i.e. $8\,\sigma$ at $\beta^* = 65$ cm and $\gamma\epsilon = 2.5\,\mu$m), thanks to the BBLR mitigation with octupoles at high telescopic index. Similar activities took place in MD4, but using instead more intense 8b4e bunch trains with up to 1.6×10^{11} p/b (see Section 3.5). Finally, the few instabilities observed during the full MD program, and dedicated collective effect related studies are summarized in Section 3.6.

3.2 Optics measurements and corrections

The OP mechanics of the full hypercycle was demonstrated in MD1 using probe beams. The first fill (fill 6800) was successfully ramped up, with the optics measured and corrected at flat-top energy ($\beta^* = 65$ cm), and the optics re-measured (but not corrected) at the end of the squeeze

($\beta^* = 25$ cm). The β-beating measured at flat-top energy in the first fill, before and after correction, is reported in Fig. 1 for Beam 1 (where two β-beating correction knobs were actually needed to further optimize the optics after the coupling correction in between), and in Fig. 2 for Beam 2. After correction, the peak β-beating was found in the range of 10-15 % for B1H (with worst cases identified in the middle of sectors 81 and 45), 5 % for B1V, and 10 % for B2H and B2V.
The optics measurements conducted at $\beta^* = 25$ cm are shown for both beams in Fig. 3, with no further global correction applied (only the EoR optics correction knobs). A knob for Beam 1 was nevertheless calculated at 25 cm (`2018_hightele_global_25cm_beam1`), expected to be very efficient although not trimmed in (the squeeze was planned to be played only once for demonstrating the OP mechanics), while the optics quality was found already quite good for Beam 2.
For preparing the second fill and validating the optics correction, the global β-beating (and coupling) knobs (`2018_hightele_global_beam1`, `2018_hightele_global2_beam1`, `2018_hightele_global_beam2`, `2018_hightele_global_coupling_beam1`, and `2018_hightele_global_coupling_beam2`) were then incorporated backward in the ramp at $\beta^* = 2$ m, corresponding to the last non-telescopic optics of the ramp (see Tab. 1). The β-beating was measured accordingly in the ramp of the second fill, with snapshots taken at ~ 2.7 TeV for Beam 1 and ~ 3.1 TeV for Beam 2 ($r_{\text{Tele}} \sim 1$), then ~ 4.9 TeV ($r_{\text{Tele}} \sim 2$) for both beams, and at flat-top energy ($r_{\text{Tele}} \sim 3$). The results obtained are shown in Fig. 4 if the phase method is used to reconstruct the β-functions, and Fig. 5 if the amplitude method is used instead[2]. Although these two methods give sensibly different results for the insertions, the orders of magnitude to keep in mind are a peak β-beating

- of about 20 % in the arcs (vs. 15 % for the nominal ramp), both at the intermediate telescopic index of 2 (4.9 TeV), and at ~ 3 TeV at the very beginning of the tele-squeeze, but with β^* being already squeezed down to 2 m at IP1 and IP5 while the persistent current induced field imperfections are still sizable in the superconducting magnets,

- in the range of 10-15 % in critical insertions such as IR3, IR6, and IR7, if one keeps in mind the systematic measurement errors of -7 % (± 5 % r.m.s.) for the amplitude method when it is applied to the wide aperture or stripline insertion BPMs [7].

Despite the very decent β-beating re-measured at flat-top energy, the optics control degradation in the ramp is due to the simple linear incorporation of the optics correction knobs, from 0 to 1, between 2.7 TeV and 6.5 TeV. This may require an optics correction for at least one intermediate energy if such an aggressive CRDS would be deployed in the LHC, namely: with $r_{\text{Tele}} = 3.1$ at the end of the ramp and the telescopic squeeze starting at 2.7 TeV, to be compared with an EoR tele-index of $r_{\text{Tele}} \sim 2$ and a telescopic squeeze starting at $\sim 4 - 4.5$ TeV for the CRDS presently discussed for Run 3.

[2]The so-called amplitude method is based on the oscillation amplitude: $\beta \propto amplitude^2$. In this case, the BPMs' calibration errors bias directly the measured β-functions. At standard BPMs, the BPM calibration errors induce optics measurement errors of about ± 3 % r.m.s., with a priori no systematics, while the wide aperture and stripline BPM calibration errors amplify this inaccuracy up to about ± 5 % on top of a systematic error of -7 % [7].
The so-called phase method, or N-BPM method, is described in [8]. It combines the β-functions calculated from multiple BPM combinations within a certain range around a given BPM (BPM_1). For a single combination of 3 BPMs, the measured β-function is related to the phase measurement as follows: $\beta \propto \frac{\cot(\phi_{12,\text{meas}}) - \cot(\phi_{13,\text{meas}})}{\cot(\phi_{12,\text{mod}}) - \cot(\phi_{13,\text{mod}})}$, where ϕ_{ij} is the phase advance between BPMs i and j, and the subscripts "meas" and "mod" refer to the measured and nominal values. Using this method, a reliable estimate of the phase advance, and de facto of the β-beating, measurement accuracy is very difficult for single kick excitation.

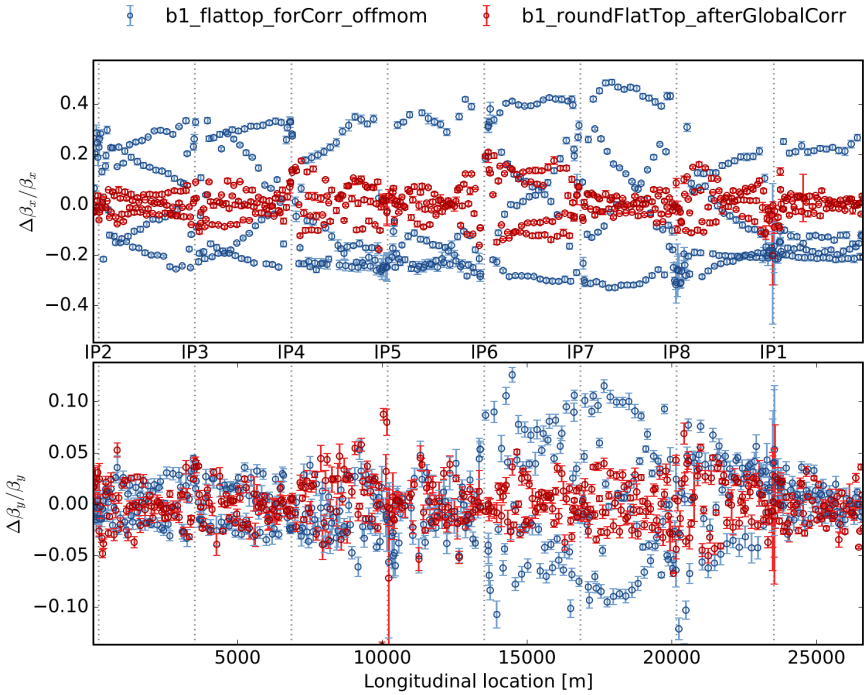

(a) : Before (blue) and after (red) the first global correction

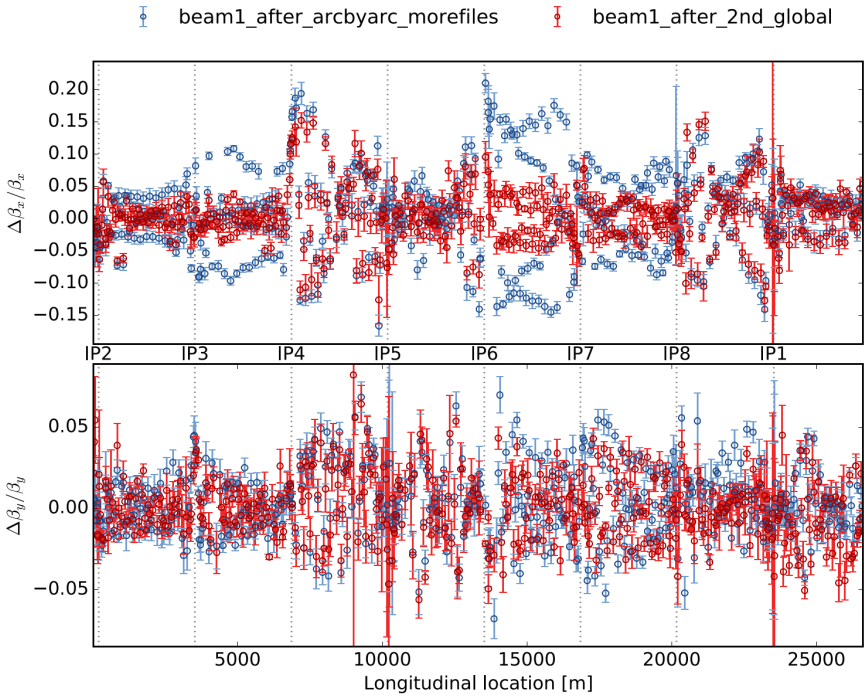

(b) : Before (blue) and after (red) the second global correction

Figure 1: Optics measurements taken for Beam 1 at the end of the ramp in the first fill ($\beta^* = 65$ cm with $r_{\mathrm{Tele}} \sim 3$), before and after the first global β-beating (and coupling) correction (top picture), and before and after the second global β-beating correction (bottom picture).

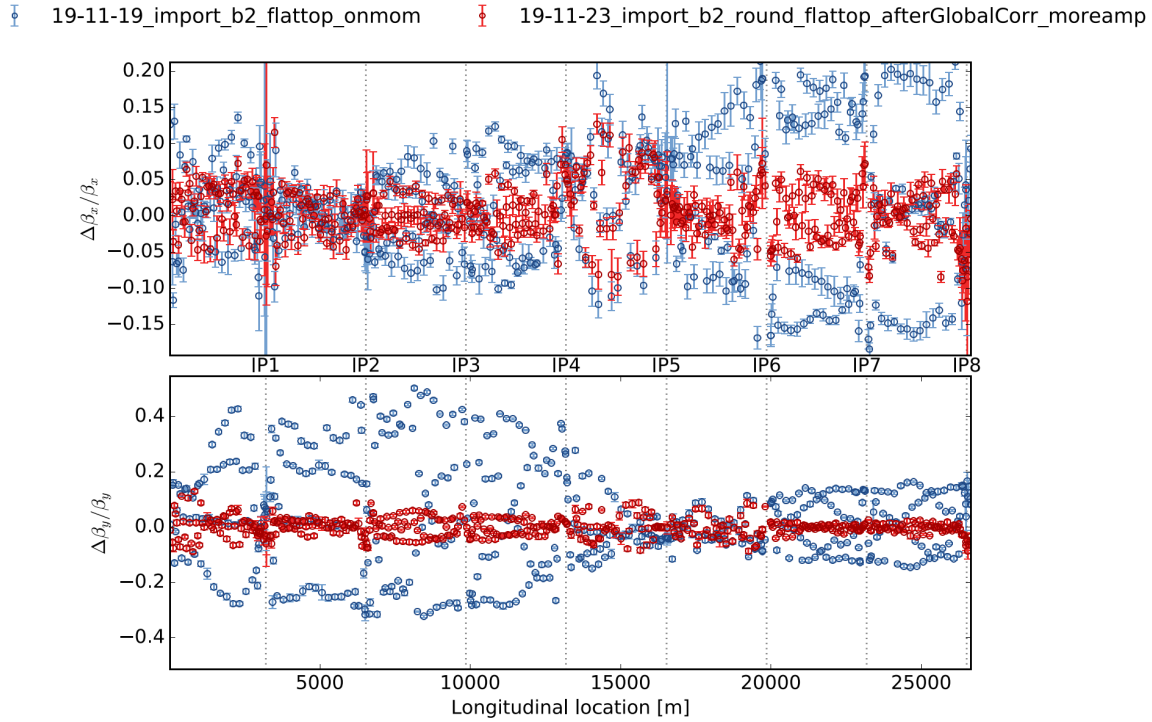

Figure 2: Optics measurements taken for Beam 2 at the end of the ramp in the first fill ($\beta^* = 65$ cm with $r_{\mathrm{Tele}} \sim 3$), before (blue) and after (red) global β-beating (and coupling) correction.

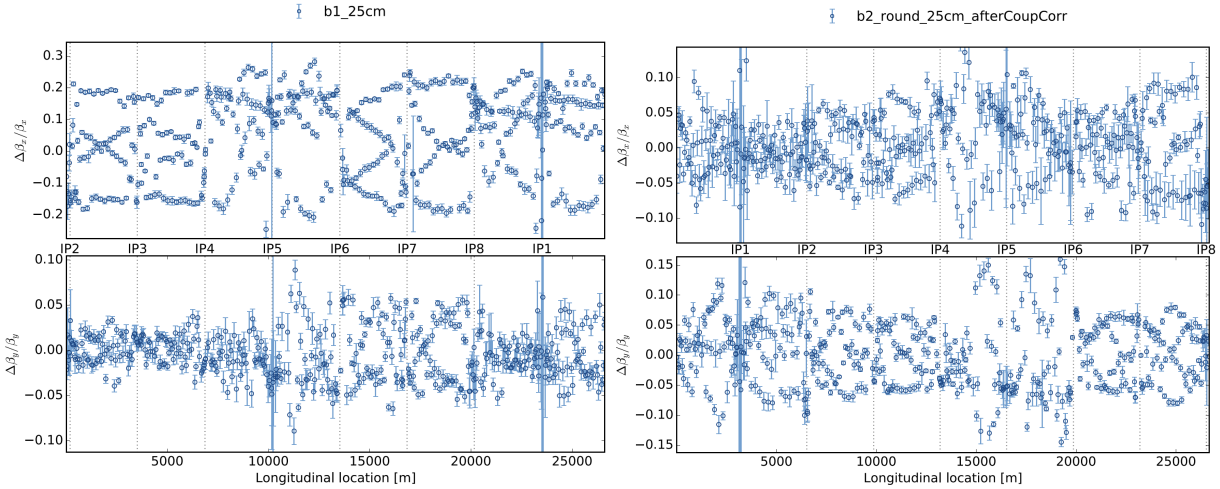

(a) : Beam 1 (b) : Beam 2

Figure 3: Optics measurements for both beams taken at the end of the squeeze in the first fill ($\beta^* = 25$ cm with $r_{\mathrm{Tele}} \sim 3$), with no correction applied (except the ones incorporated at $\beta^* = 65$ cm).

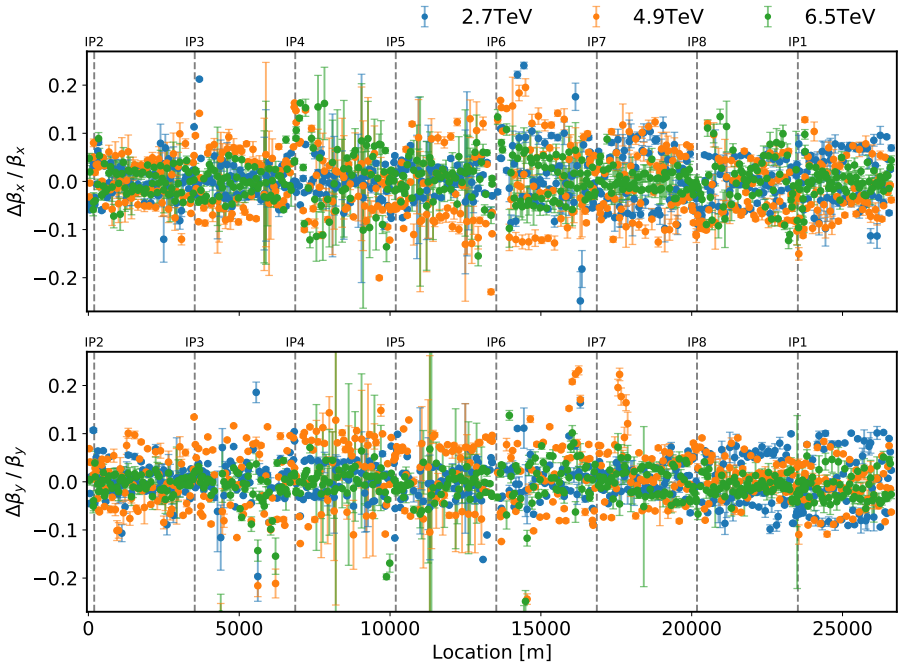

(a) Beam 1

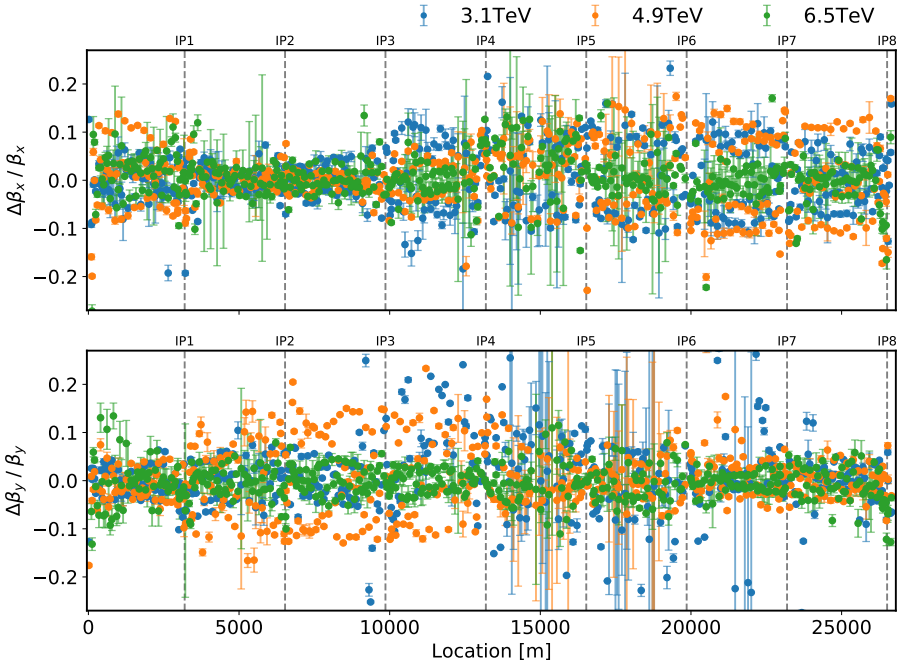

(b) Beam 2

Figure 4: Optics measurement snapshots taken on the fly for both beams during the ramp for the second fill. The phase method (N-BPM method [8]) is used to reconstruct the optics. The two intermediate energy values are approximate due to the difficulty of synchronizing the AC dipole kicks with the energy ramp, and roughly correspond to a telescopic index of 1 and 2, respectively (see Tab. 1).

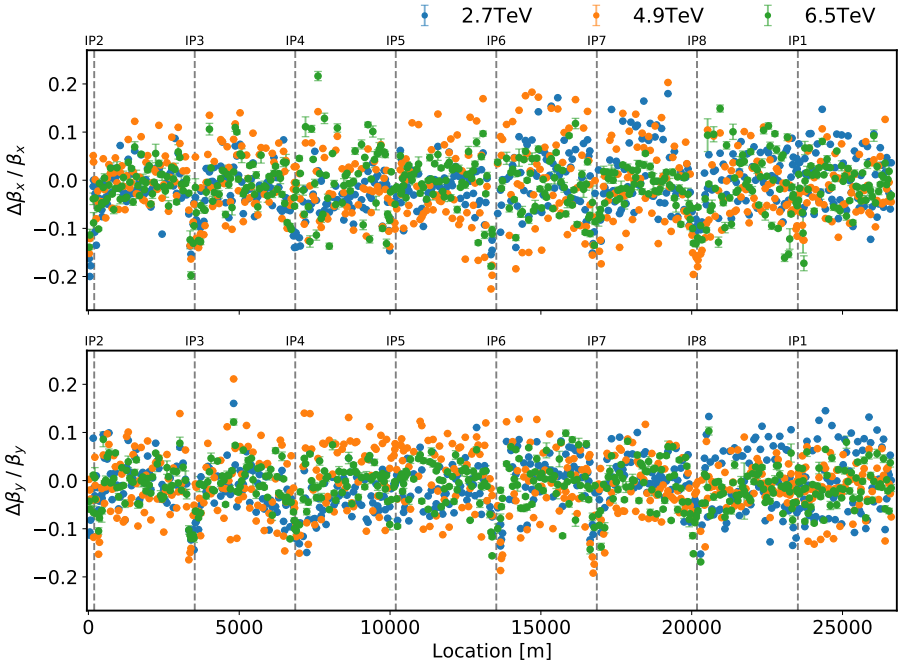

(a) Beam 1

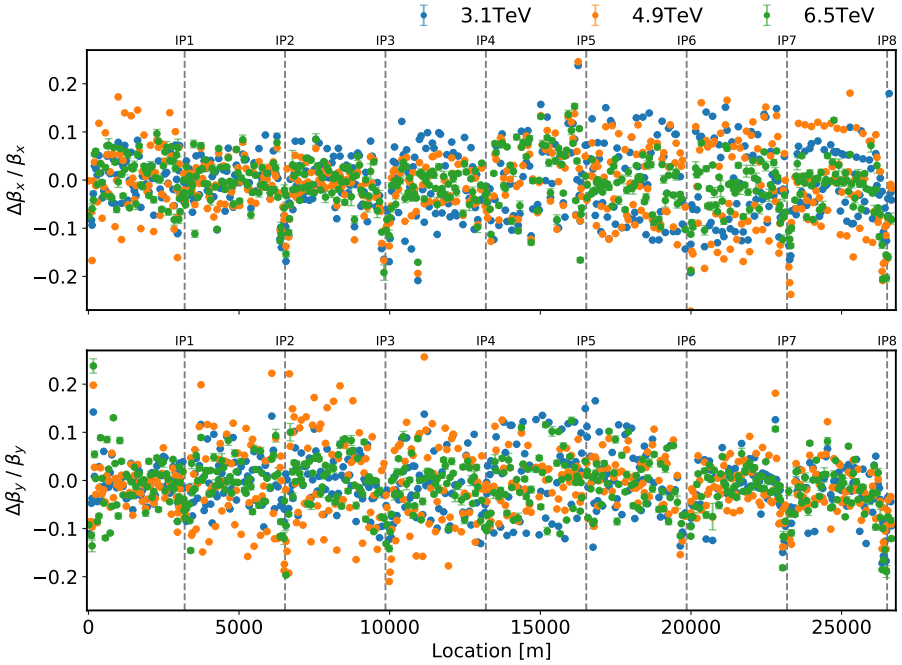

(b) Beam 2

Figure 5: Optics measurement snapshots taken on the fly for both beams during the ramp for the second fill. The amplitude method is used to reconstruct the optics. The two intermediate energy values are approximate due to the difficulty of synchronizing the AC dipole kicks with the energy ramp, and roughly correspond to a telescopic index of 1 and 2, respectively (see Tab. 1). The negative β-beating peaks measured in most of the insertions are an artefact of the method coming from calibration errors in the wide aperture and stripline BPMs hosted in the LHC IRs, which leads to an artificial reduction of the measured β-function by -7 % (syst.) $\pm$5 % (r.m.s.) [7].

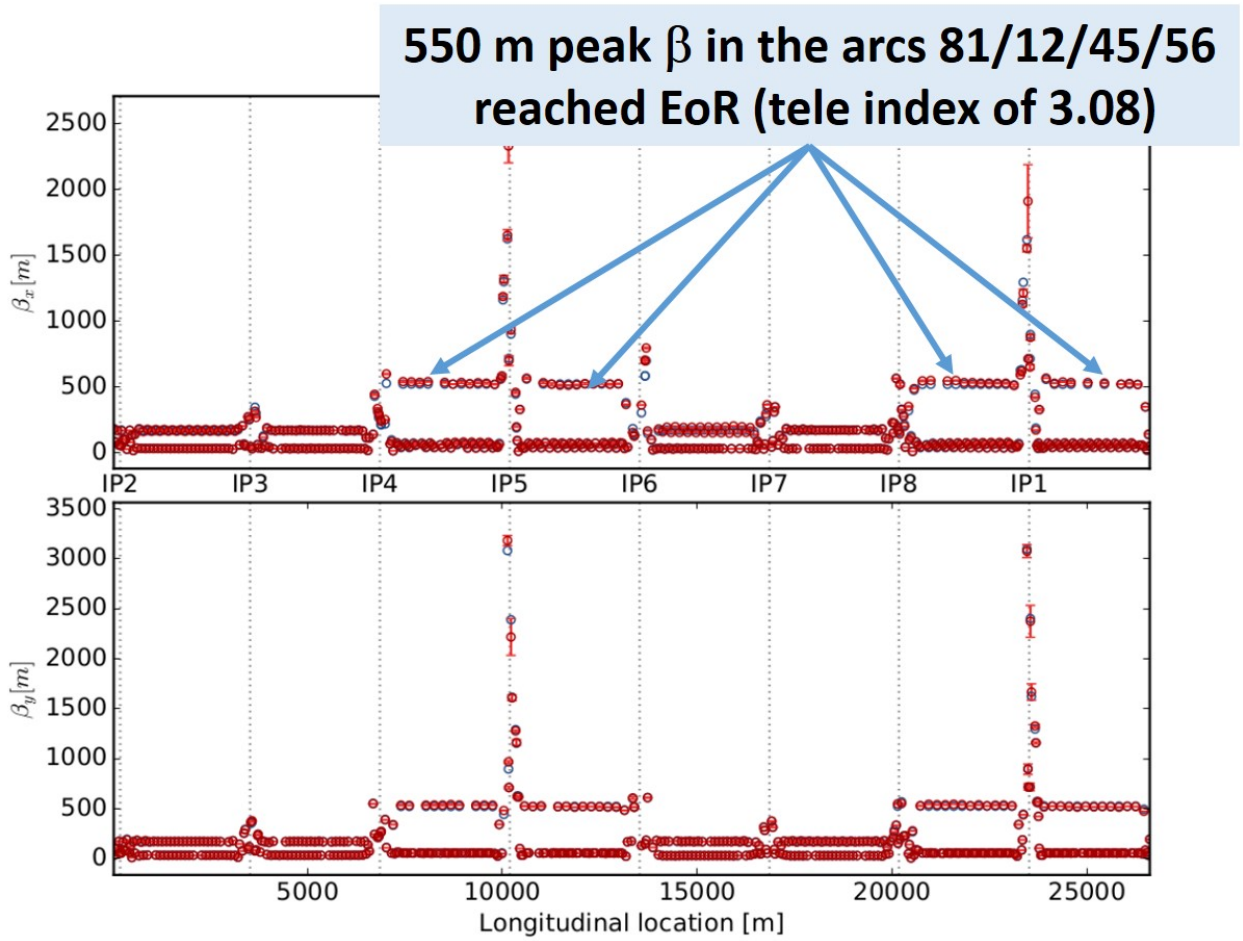

Figure 6: Optics measurements after correction at the end of the ramp ($\beta^*_{\rm Tele} = 65$ cm with $r_{\rm Tele} = 3.08$), leading to direct and crossed anharmonicity terms which are almost tripled and doubled, respectively, at constant MO current.

The quality of the EoR optics is also nicely illustrated in Fig. 6 showing the absolute measurement of the β-functions after correction, in particular with peak β-functions reaching 550 m in the four arcs adjacent to IR1 and IR5, and leading to an amplification of the Landau damping efficiency by a factor of almost 2 and 3, for the positive and negative MO polarity, respectively (see next section).
Other standard activities related to the commissioning of a new ramp did also took place, such as tune and coupling feed-forward from one ramp to the other. More details on these aspects can be found in [9].

3.3 Octupole threshold in the ramp together with collimation activities

The added value of the CRDS in terms of octupole thresholds was demonstrated in MD2 using setup beams ($\lesssim 3 \times 10^{11}$ p/beam), in parallel with the validation of the new hypercycle for collimation and machine protection. In this respect, two ramps were played with octupole functions of either polarity, ending up at ± 200 A at flat-top energy (fills 6978 and 6979, respectively).
The first ramp was played using the positive MO polarity (see the ramp function in Fig. 7), and with a filling scheme consisting of two nominal bunches with $\sim 9.0 \times 10^{10}$ p/b and 10 pilot bunches. First, new TCT functions (N_σ and centers) were loaded, pre-calculated from MADX. No beam activity was detected in the ramp. Loss maps successfully took place at the intermediate energies of 2.7 TeV (start of the tele-squeeze) and 4.9 TeV ($r_{\mathrm{Tele}} \sim 2$), showing no peculiar anomalies. Beam-based TCT alignments were conducted at the end of the ramp ($r_{\mathrm{Tele}} \sim 3.08$), then successfully validated with a third series of loss maps. An octupole scan from $+200$ A up to $+570$ A followed (with the QFB off), showing some (manageable) impact on the lifetime of Beam 1 (down to ~ 50 h during the trims, see Fig. 8). Collisions were then established and optimized at $\beta^* = 65$ cm at all four interaction points (IP). A very weak instability was observed during the research of collisions at IP2 (see Sub-Section 3.6.1). The TCTs were re-aligned in collision, which was validated with a fourth and last series of loss maps. While in collision, the octupole polarity was successfully reversed (no instability), the beams re-separated with 6 σ's, and the octupole threshold found in the range of -25 A (with negative MO polarity, see Fig. 7). This fill ended up with a programmed dump. As the bunches had experienced instabilities during ADJUST possibly affecting their distribution and consequently the instability threshold, the measurement was repeated in the next MD block (Fill 7173), and the threshold was confirmed at -25 A.
Similar activities took place in a second fill, using the negative octupole polarity (see the MO ramp function in Fig. 9), and a filling scheme containing two nominal bunches with $\sim 1.15 \times 10^{11}$ p/b and 9 pilot bunches. In particular, the loss maps taken on the fly in the ramp still did not show any anomalies, the MO scan played at flat-top energy from -200 A down to -570 A had strictly no impact on the beam lifetime (see Fig. 10), the collisions were found immediately, the MO polarity successfully reversed when colliding, and the MO threshold (with re-separated beams) found to be around 100 A (with positive polarity, see Fig. 9). The fill ended up with a successful asynchronous beam dump test.
The large difference (by a factor of ~ 4) between the two MO thresholds can be explained by

- the difference in terms of bunch charge between the two fills ($\sim 30\,\%$),
- the fact that the direct and cross-anharmonicity coefficients are amplified differently by the end-of-ramp telescopic optics [by a factor 2.89 and 1.95, respectively, at $r_{\mathrm{Tele}} = 3.08$, see Eq. (1)], while the first coefficient, which is positive, is the relevant detuning term when the octupole polarity is negative (for Landau damping coherent tune shifts with negative real parts coming from the resistive impedance of the collimators), and conversely for the cross-anharmonicity term which is negative,
- the typical factor of ~ 1.7 [10], for Gaussian beams and standard (non-telescopic) LHC optics, in favor of running the machine with the negative polarity of the octupoles. This polarity is indeed better-suited to deal with the single bunch collective effects driven by the LHC impedance which is largely dominated by the resistive contribution of the collimators (complex tune shifts with largely negative real parts).

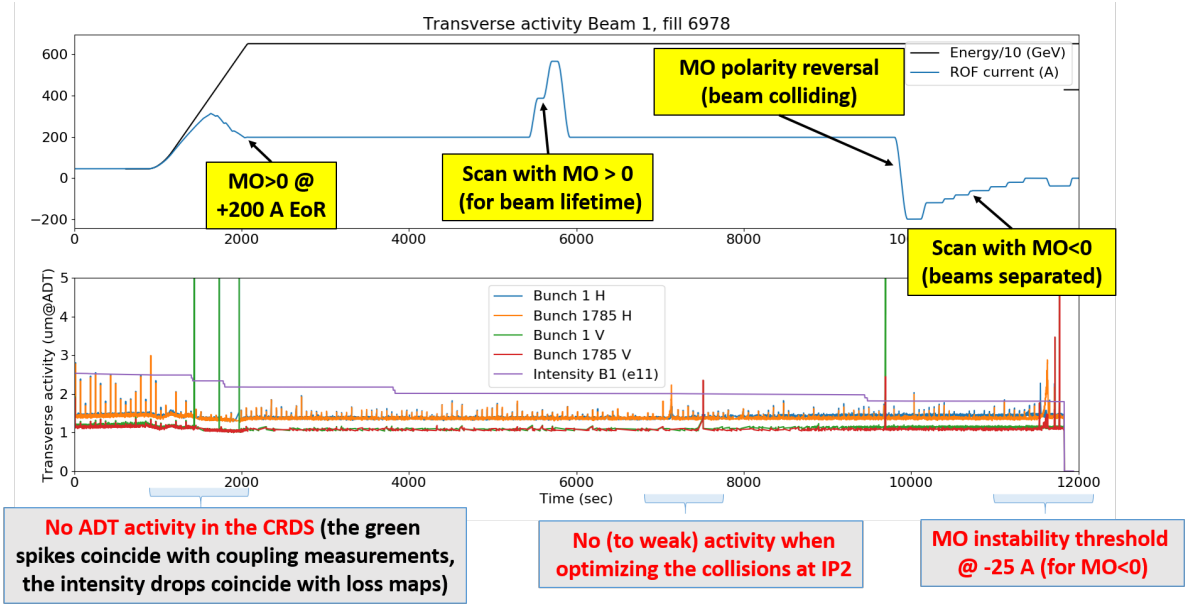

Figure 7: MO ramp function (in the case of the positive polarity) used for single-bunch in MD2, beam activity observation in the ramp, and measurement of the MO threshold at 6.5 TeV with negative polarity (at $\sim 0.90 \times 10^{11}$ p/b).

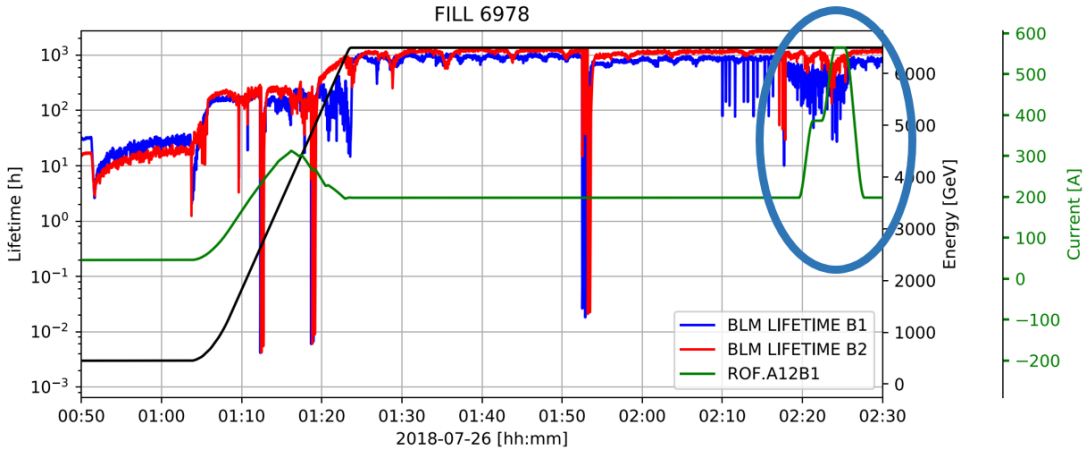

Figure 8: Beam lifetime versus octupole current for the first ramp with the MO polarity set to positive (fill 6978), including a dedicated scan at flat-top energy at constant MO polarity (with the tune feedback off). The 3 lifetime deeps coincide with loss map measurements at 2.7 TeV, 4.9 TeV and 6.5 TeV, respectively. The lifetime of Beam 1 was found to be sensitive to the MO scan at flat-top energy, with a (still reasonable) dip down to 50 h during the MO trims.

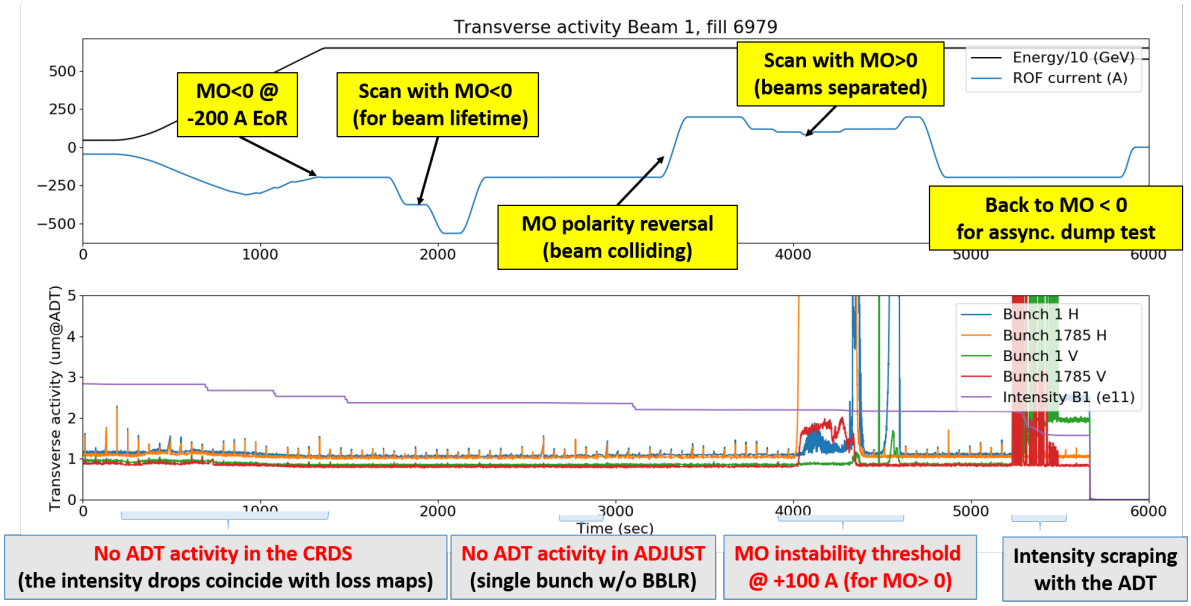

Figure 9: MO ramp function (in the case of the negative polarity) used for single-bunch in MD2, beam activity observation in the ramp, and measurement of the MO threshold at 6.5 TeV with positive polarity (at $\sim 1.15 \times 10^{11}$ p/b).

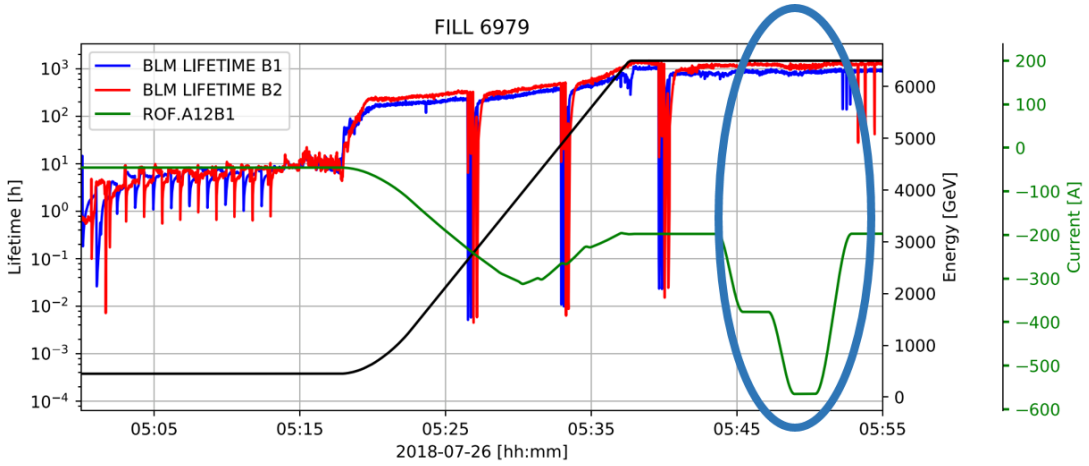

Figure 10: Beam lifetime versus octupole current for the second ramp with the MO polarity set to negative (fill 6979), including a dedicated scan at flat-top energy at constant MO polarity (with the tune feedback off). The 3 lifetime deeps coincide with loss map measurements at 2.7 TeV, 4.9 TeV and 6.5 TeV, respectively. The lifetime of both beams was found insensitive to the MO scan at flat-top energy.

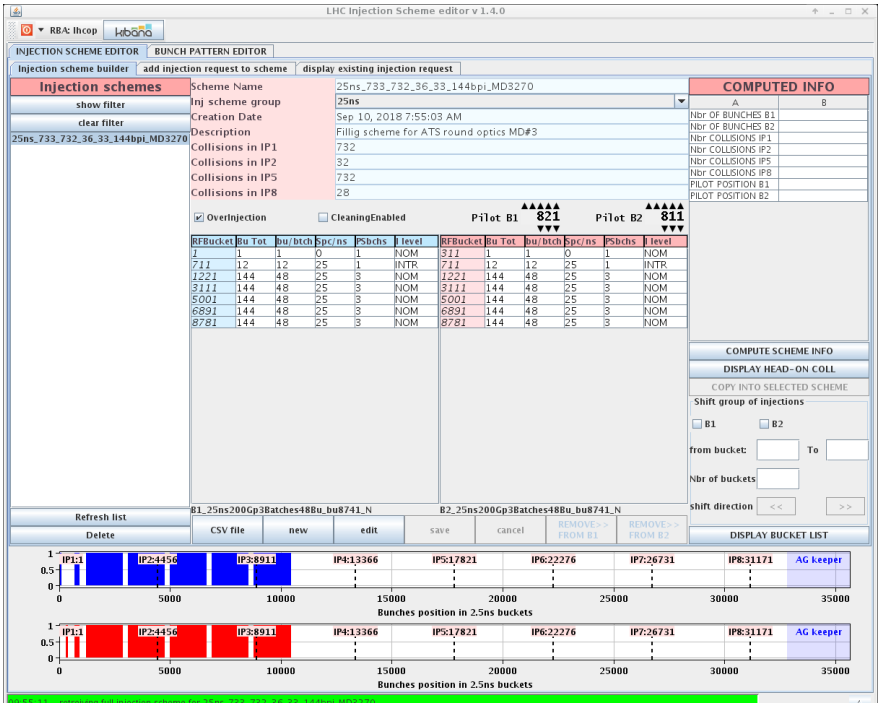

Figure 11: Filling scheme with 733 nominal bunches in MD3.

3.4 Intensity ramp up and BBLR mitigation with octupoles

3.4.1 Intensity ramp up procedure, and filling scheme

At the beginning of the MD block 3, a few hours of machine time were successfully used for the re-validation of the hypercycle (fill 7151). The intensity ramp up took place in three consecutive steps (fills 7171, 7173, and 7174), namely:

- **Step 1** with 1 non-colliding (n.c.) bunch (INDIV) for tune monitoring, a first train of 12 bunches (all colliding at IP1 and IP5), and one BCMS train of 48 colliding bunches, which made a total of 61 nominal bunches,
- **Step 2** with 1 n.c. bunch (INDIV), 12 (colliding) bunches and 2 SPS injections of 144 colliding bunches each, that is 301 bunches in total,
- **Step 3** idem as above but with 5 SPS injections, that is 733 bunches in total (see Fig. 11 for the details of the filling scheme).

The chromaticity was set up to 10 units. Step 1 was run with the positive polarity of the octupoles (same ramp function as in MD2, see Fig. 7), which was then reversed in collision for the study the BBLR mitigation with octupoles, in particular the crossing angle reach (see Sub-Section 3.4.3). To be noted that the non-colliding bunch was found unstable for each beam during the polarity reversal, as expected, at a MO current of about 50 A (see Sub-Section 3.6.2). The second and third fills (with 301 and 733 bunches, respectively) were then played directly with the negative polarity of the octupoles, using a new pre-calculated ramp function ending up at -350 A at flat-top energy (see Fig. 12), i.e. with an EoR current increased with respect to the single bunch tests of MD2 in

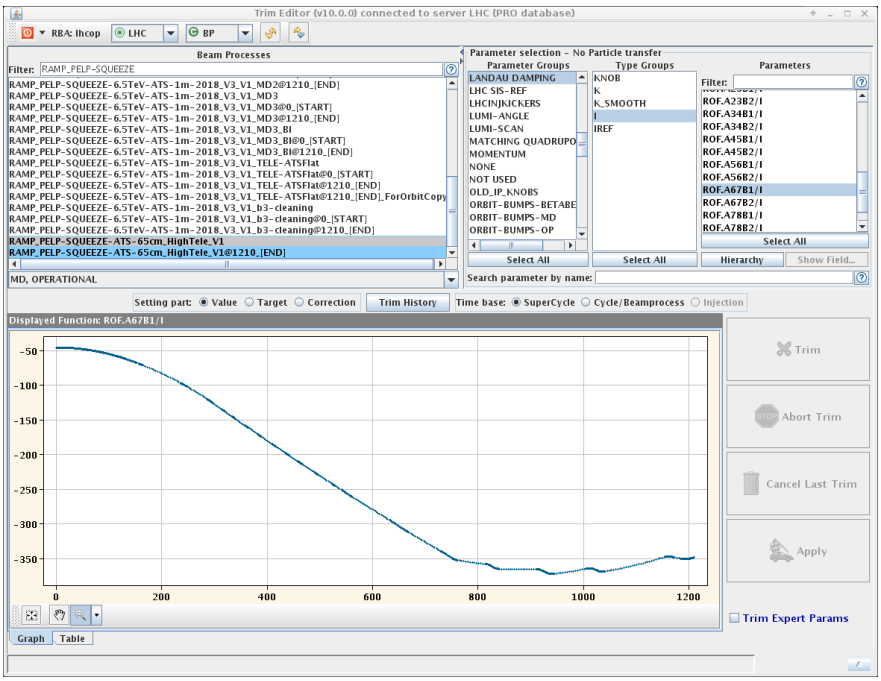

Figure 12: Octupole ramp function with negative polarity used in MD3 for the steps 2 and 3 of the intensity ramp up (MO current of -350 A EoR).

order to counter-balance the contribution to the tune spread coming from the BBLR interactions. No instability was observed in Step 2 and Step 3, including during the standard (fast) ADJUST beam process (with $\beta^* = 65$ cm and a half-crossing angle of $120\,\mu$rad). To be noted that other special tests were run at the end of the MD, with a reduced crossing angle ($95\,\mu$rad instead of $120\,\mu$rad) and/or lower current in the octupoles (up to -200 A instead of -350 A), showing as well no instability for a fast (standard) collapse of the parallel separation. On the other hand, some instabilities were triggered when lengthening on purpose the collision beam process, at a critical parallel separation in the range of $1.5 - 2.0\,\mathrm{beam}\,\sigma$'s [11] (see also Sub-Section 3.6.3 for more details).

3.4.2 Main observations (transmission in the ramp, emittance preservation, heat load, luminosity)

The beam lifetime was found rather good in the ramp, although showing a net reduction down to 50-100 h for Beam 1 towards the end of the ramp (see Figs. 13 for Fill 7174 with 733 nominal bunches), but with a very good emittance measured in the range of $1.5 - 2\,\mu$m at flat-top energy (see Fig. 14). Comparing the heat load measured for a typical fill in nominal operation and for the last MD fill with 733 nominal bunches, no specific features have been identified, despite the complete different optics in four arcs of the ring (see Fig. 15). Bringing the beams into collision led to a luminosity in the range of $3.6 - 3.7 \times 10^{33}\,\mathrm{cm}^{-2}\mathrm{s}^{-1}$ ($\beta^* = 65$ cm, $\theta_X/2 = 120\,\mu$rad, $N_b = 732$ collisions, $N \sim 10^{11}$ p/b, $\gamma\epsilon \sim 2\,\mu$m). This value scales rather precisely with the peak luminosity of $2 \times 10^{34}\,\mathrm{cm}^{-2}\mathrm{s}^{-1}$ which was reached in operation at the beginning of stable beam for the typical beam and optics parameters used in 2018 (see Fig. 16).

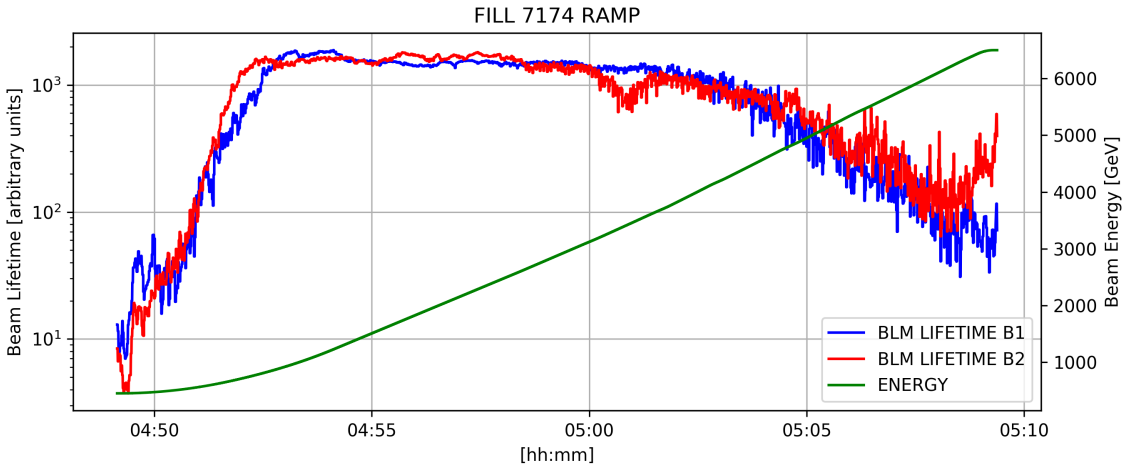

Figure 13: Beam lifetime in the ramp for fill 7174 (733 nominal bunches).

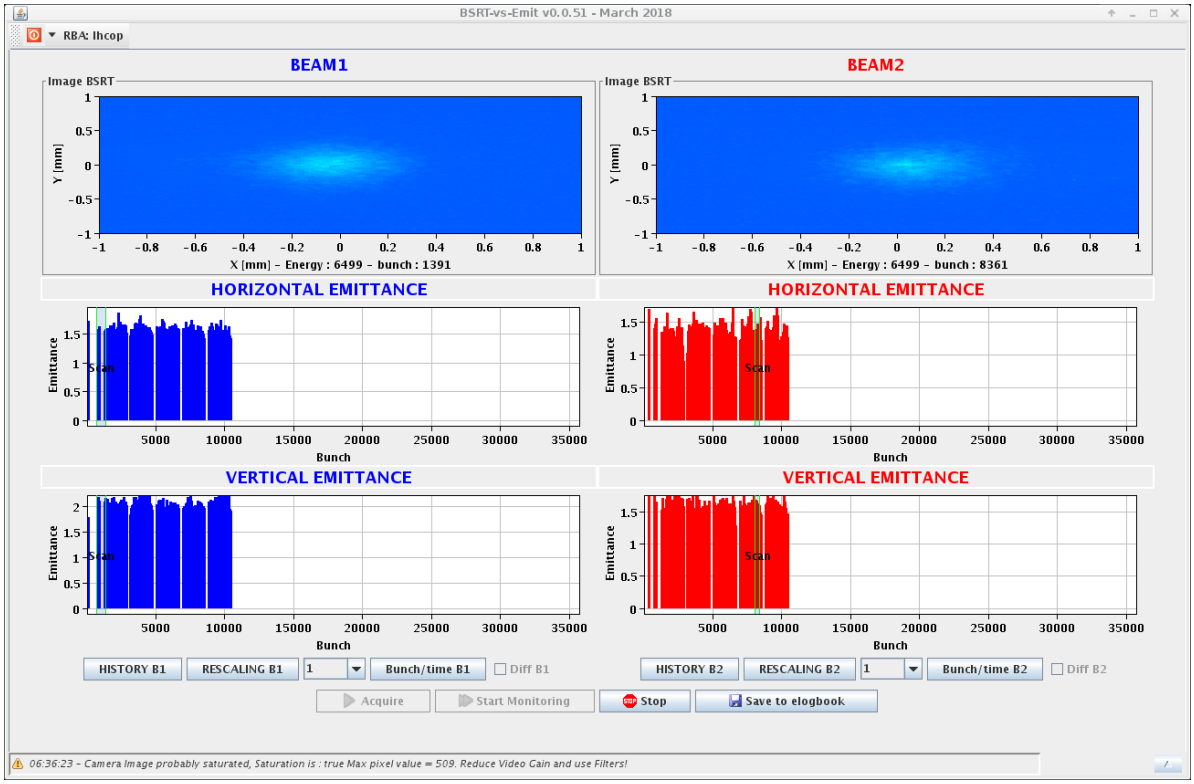

Figure 14: Beam emittance measured at the end of the ramp for fill 7174 (733 nominal bunches).

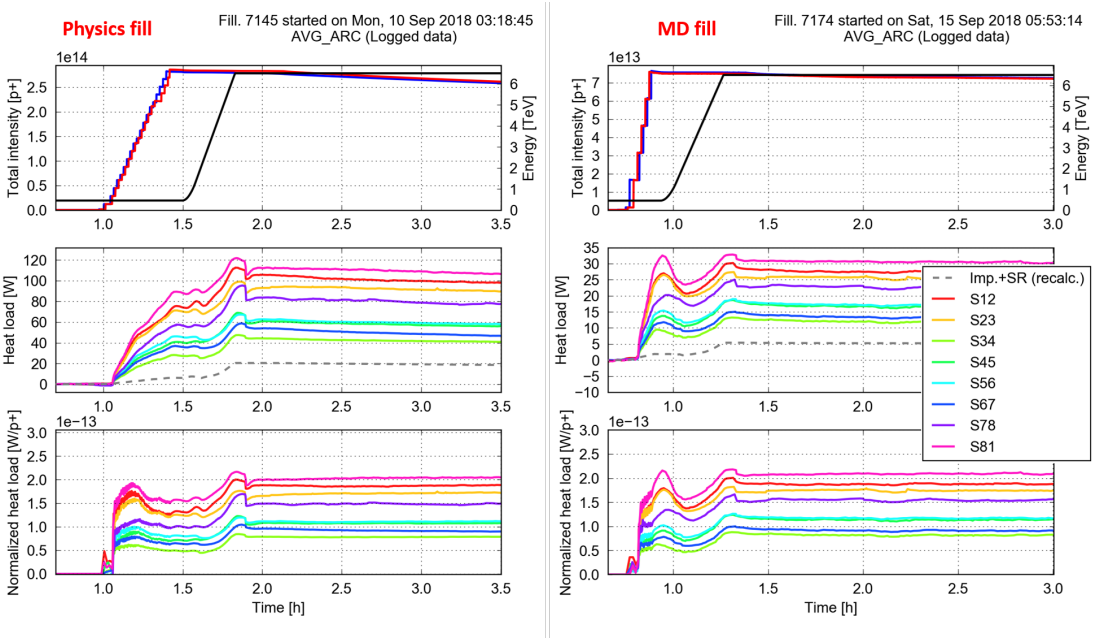

Figure 15: Heat load for a typical physics fill (left) and for fill 7174 with 733 nominal bunches.

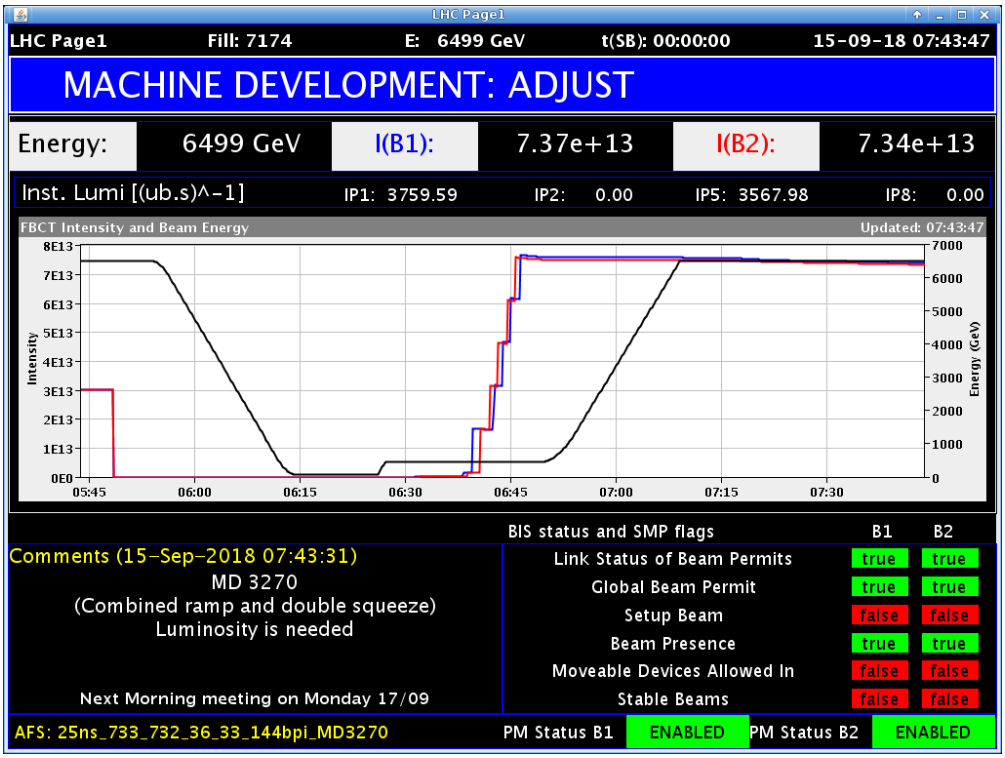

Figure 16: Beam transmission in the ramp and luminosity at the beginning of stable beam for fill 7174 (733 nominal bunches, with 732 colliding at IP1 and IP5).

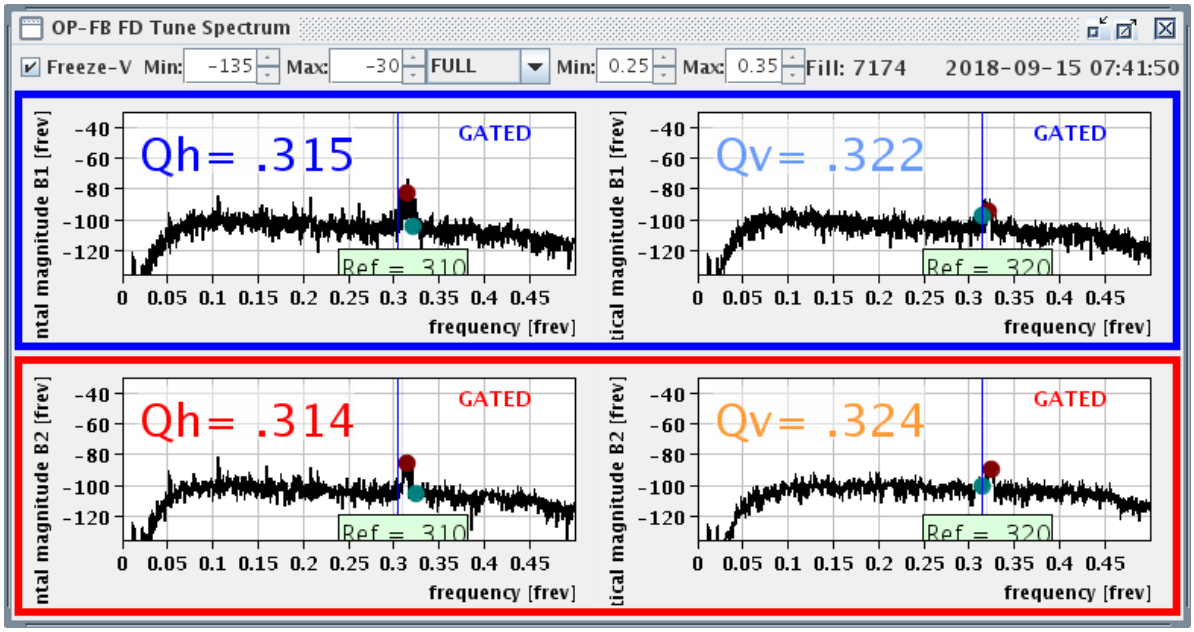

Figure 17: Optimal betatron tunes in collision for MD3 with the MOs set to -570 A (negative polarity), and a half-crossing angle of 100 μrad.

3.4.3 BBLR mitigation with octupoles and crossing angle reach

Using the lattice octupoles as a mitigation tool for the BBLR effects, the crossing angle reach was quantified in the first step of the intensity ramp up (with 12+48=60 colliding bunches, and the MO polarity chosen positive in the ramp, see Sub-Section 3.4.1). For this purpose, the octupole polarity was first reversed to negative with the beams colliding, and the MO current pushed down to -570 A. The half-crossing angle was then reduced by small steps of 10 μrad, from 120 μrad (10.2 σ for $\beta^* = 65$ cm and a beam emittance of $\gamma\epsilon = 2.5\,\mu$m) down to 90 μrad (7.6 σ), while reoptimizing the betatron tunes whenever needed (which led to a positive tune shift in the range of $\Delta Q \sim 0.003 - 0.004$ along the diagonal at low crossing angle, taking as reference the working point used in nominal operation with positive MO polarity, see Fig. 17). The half-crossing was finally fine-tuned to 95 μrad (8.1 σ) in order to restore the typical lifetime of about 35 h generally observed in stable beam operation (see Fig. 18).
At the fixed half-crossing angle of 95 μrad, the signature of the BBLR interactions was then obtained by looking at the lifetime of each individual bunches as a function of the MO current, more precisely at the so-called effective cross-section of each individual bunch (loss rate normalised to luminosity compared to the burn-off limit of 80 mb). The results obtained are illustrated in Fig. 19, for a selection of 5 representative bunches, namely the so-called pacmam 1, pacmam 2, intermediate 1, intermediate 2 and regular bunches located at the two extremities, at half-distance from the center, and at the center of the BCMS train, respectively. While the burn-off limit is reached for all selected bunches at an octupole current of -570 A, the lifetime degradation when increasing the MO current (and reversing the polarity) is clearly BBLR dependent, with the worst case reached for the central bunch (with maximum number of BBLR encounters) and the so-called bunch intermediate 2 (located at half-distance between the center and the tail of the BCMS train).

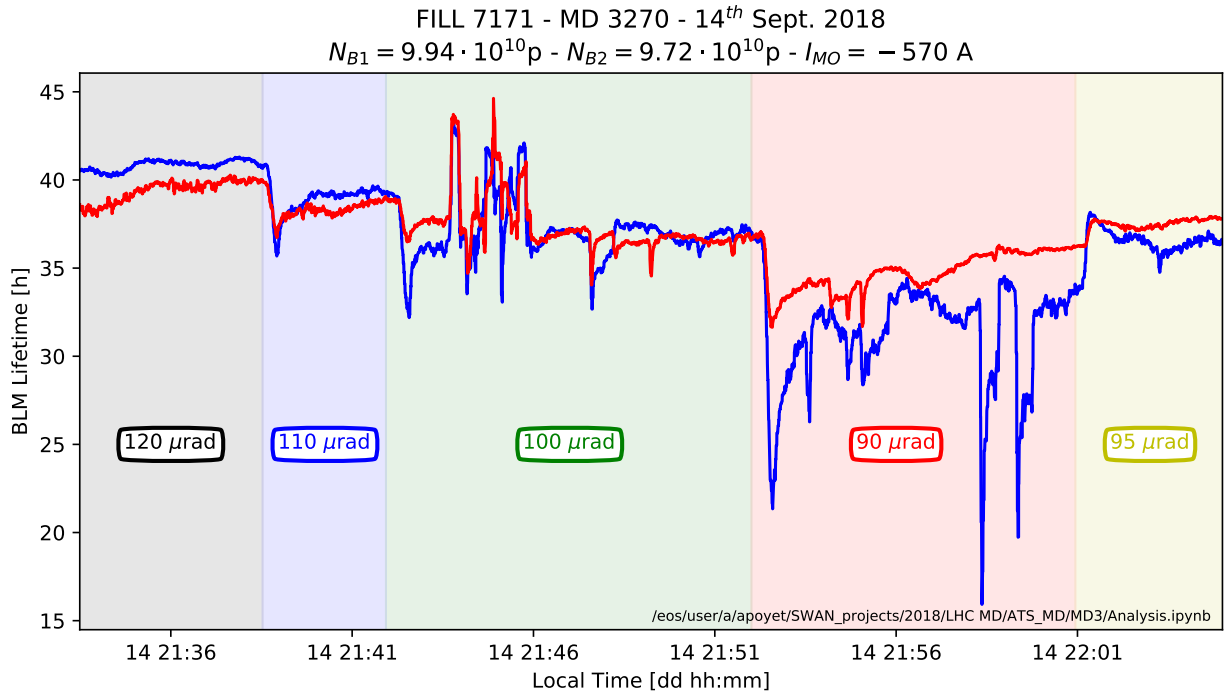

Figure 18: Crossing angle scan in collision for fill 7171 (60 colliding bunches), with the octupoles set to the maximum negative current (-570 A), and including a tune re-optimization at almost every step. In this configuration, the BBLR limit for $\sim 10^{11}$ p/b and $\beta^* = 65$ cm is in the range of $95\,\mu$rad (half-crossing angle), corresponding to a normalized crossing angle of about $8\,\sigma$ for a beam emittance of $\gamma\epsilon = 2.5\,\mu$m.

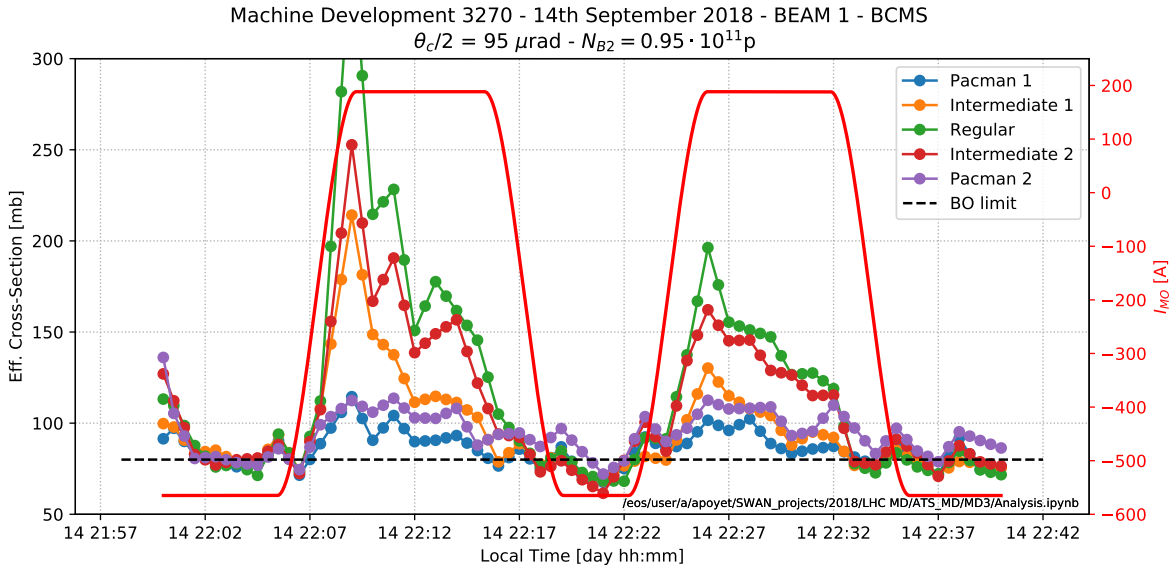

Beam 1

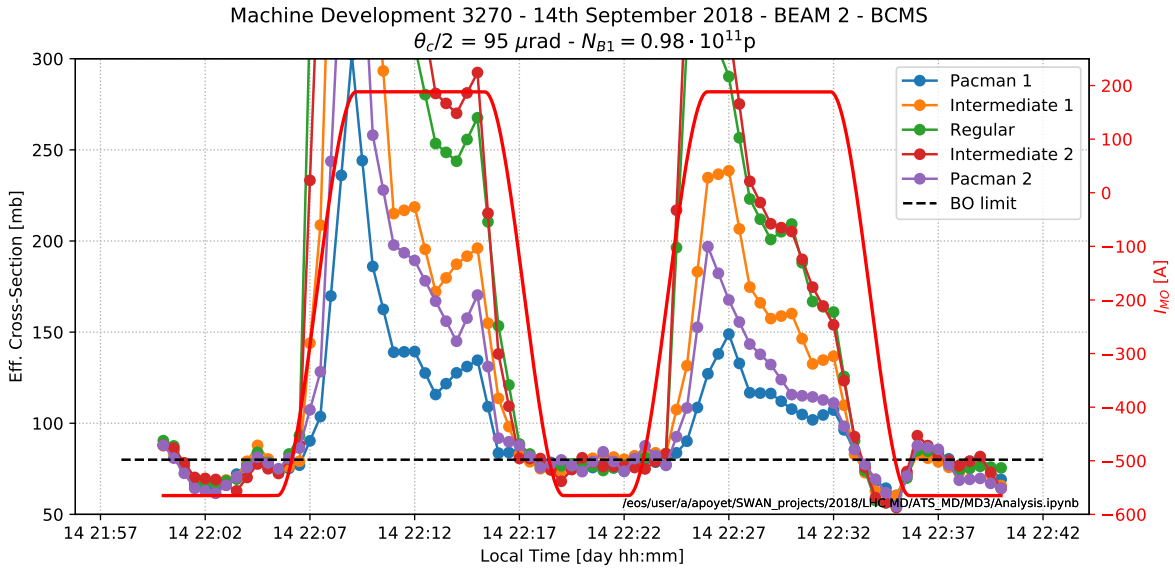

Beam 2

Figure 19: Octupole scan in collision at $\beta^* = 65$ cm, with a half-crossing angle of $95\,\mu$rad in IR1 and IR5 ($8.1\,\sigma$ for a beam emittance of $\gamma\epsilon = 2.5\,\mu$m), and $N \sim 10^{11}$ p/b: effective cross-section (i.e. loss rate normalised to luminosity) for a few bunches selected in Beam 1 (top) and Beam 2 (bottom), namely at the two extremities of the BCMS train (pacmam 1 and pacman 2), at half-distance between the extremities and the center of the train (intermediate 1 and intermediate 2), and at the center (regular).

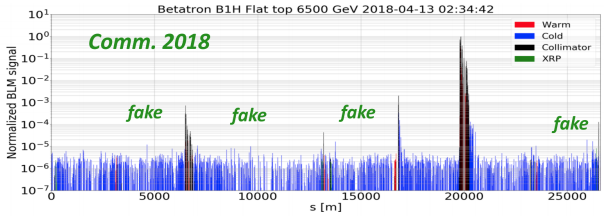

2018 commissioning EoR ($\beta^* = 1$ m)

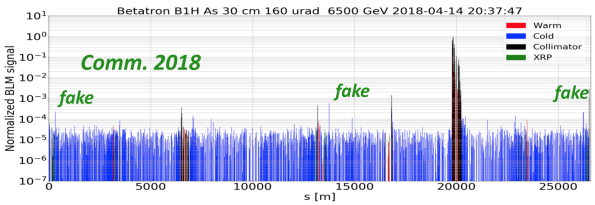

2018 commissioning EoS ($\beta^* = 30$ cm)

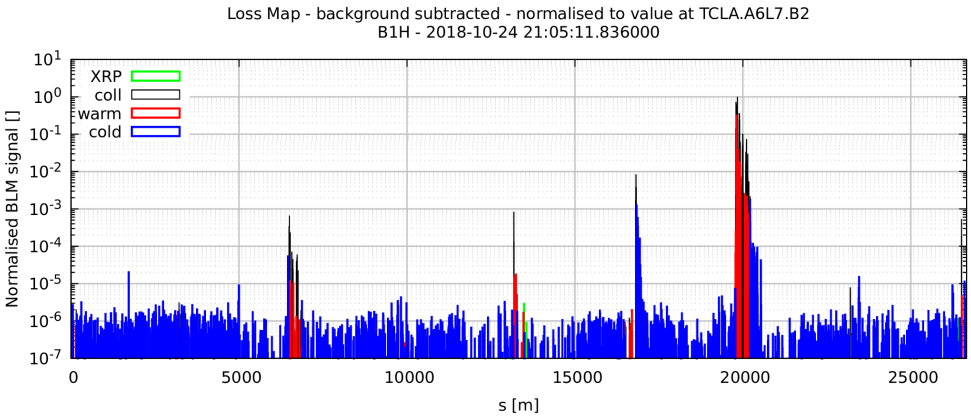

MD EoR ($\beta^* = 65$ cm)

Figure 20: Qualification loss maps for B1H for the initial 2018 beam commissioning (top pictures), taken at the end of the ramp (EoR) and the end of the squeeze (EoS) [12], compared to the B1H loss map measured at the EoR in MD4. While the losses at the triplets did not show any anomalies in MD4, the losses measured at the TCT in IR5 ($s \sim 14$ km) were found to be sensibly higher by a factor of 2 to 20 (in relative with respect to the EoS and EoR nominal cases, respectively). Losses measured in IR6 were also found higher.

3.5 Experience with high brightness 8b4e bunch trains

The program continued in MD4 in order to profit from the availability of 8b4e bunch trains of high intensity (in the range of $1.5 - 1.6 \times 10^{11}$ p/b). As in MD3, a few hours of beam time were first needed in order to re-validate the machine in this new configuration (fill 7340). This re-validation was found overall satisfactory, nonetheless showing sensibly more (but still acceptable) losses for B1H at the TCT of IR5 and in IR6 (see Fig. 20). This was possibly linked to the fact that the TCT's were set to $11\,\sigma$ in IR1 and IR5 at the end of the ramp ($\beta^* = 65$ cm) vs. $15\,\sigma$ for the nominal ramp ($\beta^* = 1$ m), i.e. with physical gaps reduced by about 10 % with respect to their nominal settings in operation.
The intensity ramp up took place in three consecutive steps, namely

- **Step1** with three 8b4e trains of 48 bunches each, following a first train of 12 colliding bunches, and a non-colliding bunch (for tune monitoring), i.e. 157 bunches in total (fill 7362).
- **Step2** with about 800 bunches of high intensity (fill 7365).
- **Step3** with the machine full of 8b4e bunch trains, for a total of about 1600 circulating bunches (fill 7366).

Due to high TCT losses observed at the end of the ramp in Step 2 (see later), it was decided to roll back to the nominal ramp for Step 3.
Contrary to MD3, the chromaticity was set to 15 units, the MO polarity kept negative, with a current pushed further down to -570 A at the end of the ramp. The injection of the three 8b4e trains (step 1) was laborious, but in the end successful after a re-steering of the transfer lines and some scraping in the SPS. The injected beam emittance was found in the range of $\gamma\epsilon = 3 - 4\,\mu$m (see Fig. 21). The first ramp was successful, with no instability, but with up to 2 % losses in average for Beam 1 (twice less for Beam 2, see Fig. 22). The corresponding lifetime dip was mitigated at flat-top energy by re-increasing the octupole current up to -500 A (big beams), and definitely cured after the Q-change, even with the octupoles back to -570 A. This seems to indicate that the losses were mainly driven by a non-optimal choice of the tune ramp function (taken nominal despite of the change of the MO polarity), rather than by the octupoles themselves. The collision beam process run smoothly, with the octupole current set to -570 A, the half-crossing angle fixed to $120\,\mu$rad in IR1 and IR5, and no sign of any instability. A quite large tune shift of $\Delta Q_{x/y} = +0.007/+0.005$ was however found to be needed for both beams, in order to reach a lifetime in between 30 h and 35 h, corresponding to an effective cross-section very close to the burn-off limit of 80 mb (see Fig. 23). No time was however left in order to precisely investigate the crossing angle reach for this type of beam.
The second step (fill 7365) of the intensity ramp up was actually part of the following MD on electron cloud studies with high intensity 8b4e beams [13]. No dedicated beam-beam and collective effect related studies were conducted during this fill. The measurement of the beam lifetime in the ramp and its comparison with the subsequent fill (played with the nominal ramp and the machine full of 8b4e bunch trains) is however relevant to show in Fig. 24. Some lifetime degradation (in relative) can be observed at the end of the ramp for Beam 2 (~ 100 h for the CRDS vs. ~ 1000 h for the nominal ramp), but no change for Beam 1 (~ 100 h at the end of both ramps). In general, both beams behaved quite similarly for the CRDS, with the CRDS sensibly better than the nominal ramp but only for Beam 1. On the other hand, the reason why the lifetime of Beam 2 is found as good as ~ 1000 h at the end of the nominal ramp is not understood.
To be noted that the end of ramp TCT losses in fill 7365 (Beam 1) were measured at level of 70 % compared to the threshold, vs. 30-40 % in IR7 (for 84 s integration time). This then justified the decision of rolling back to the nominal cycle for the last step of the intensity ramp up.
It is however worth mentioning that the TCT BLM thresholds at flat top energy are fine-tuned at the beginning of each year, based on qualification loss maps and the expected physics debris, in order to minimize the risk of magnet quenches and/or unnecessary dumps. This fine-tuning, which also involves simulations to verify that the corresponding loads on the TCT jaws are acceptable in operation, was not done for the MD; therefore, the proper alignment of TCT BLM thresholds to actual losses is not granted. Without a detailed analysis of what happened during the second ramp of MD4, when 70 % of the BLM TCT dump threshold was reached, and an estimation (even a rough one) of the load on the TCT jaws, it is not possible to draw firm conclusions. On the other hand, negligible or even non-existent losses were seen at the IR5 inner triplet in the MD qualification loss maps, despite the relatively high load on the TCT immediately upstream (see Fig. 20 for the comparison with loss maps taken for the nominal hypercycle). Hence, it is highly likely that the BLM threshold at the TCTs could have been relaxed for the MD without issues for the TCT jaws and the downstream inner triplet.

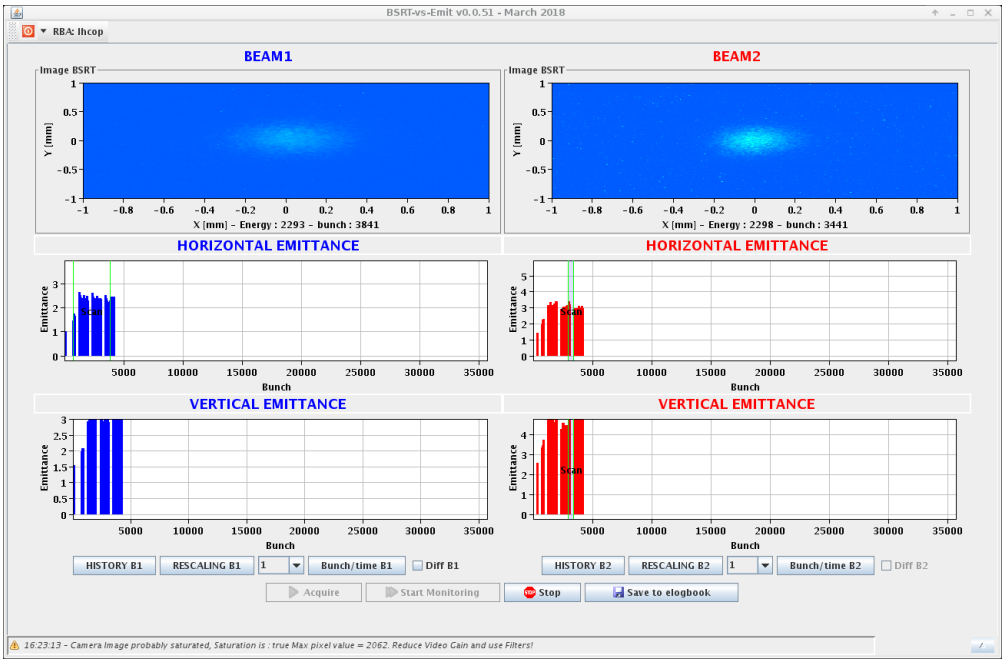

Figure 21: Beam emittance measured at injection in MD4 for 8b4e bunch trains (fill 7362 corresponding to step 1 of the intensity ramp up).

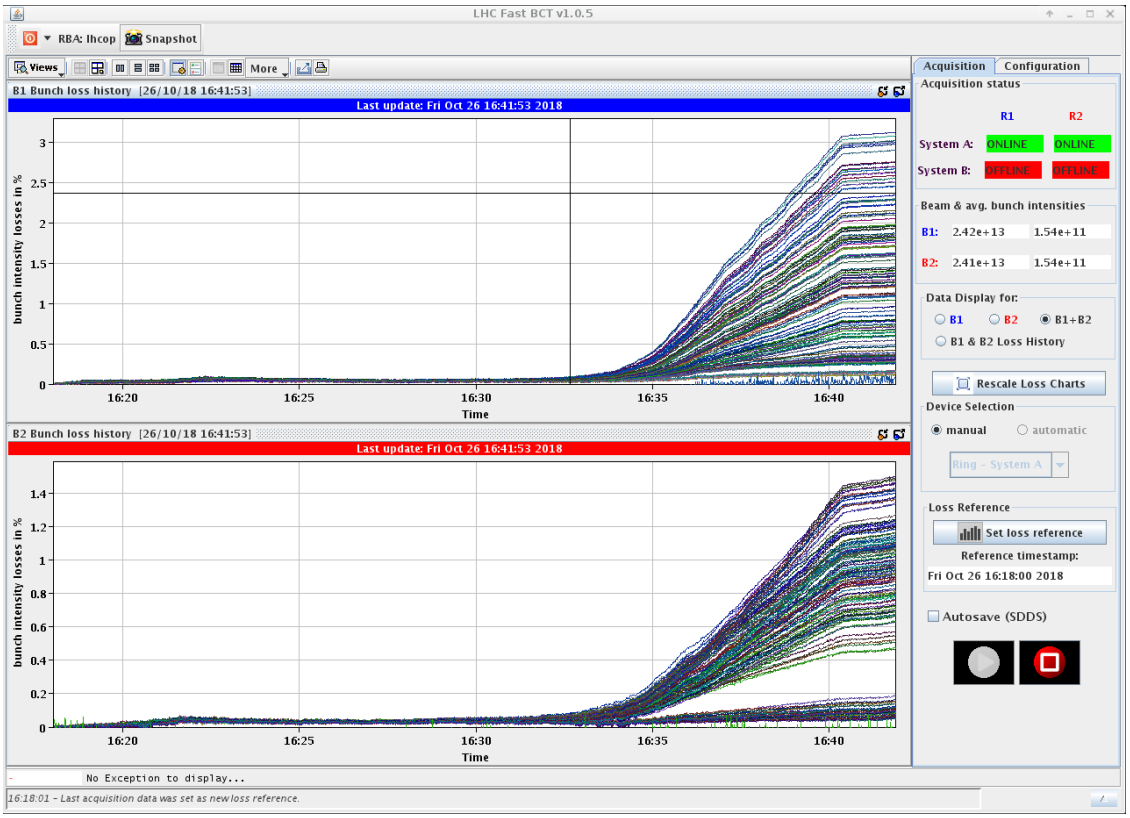

Figure 22: Accumulated losses in the first ramp of 8b4e bunch trains (fill 7362 with 157 bunches).

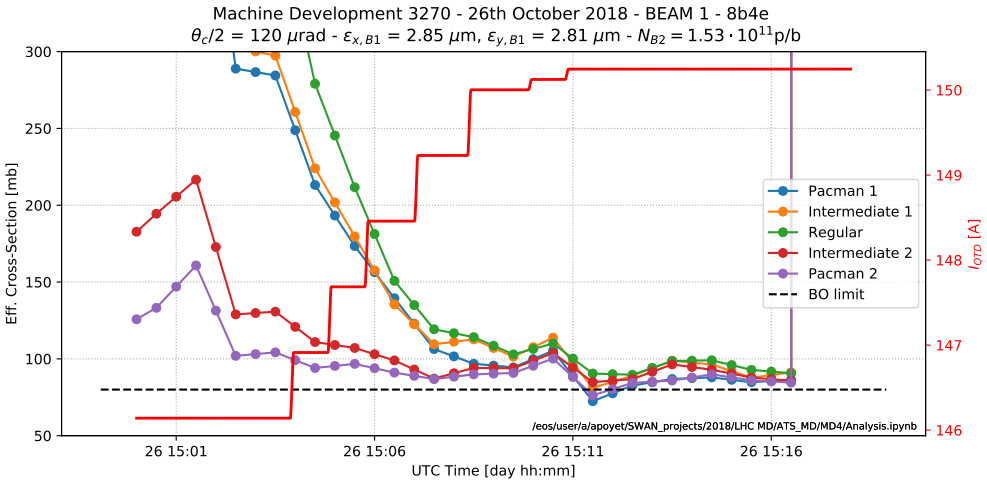

Beam 1

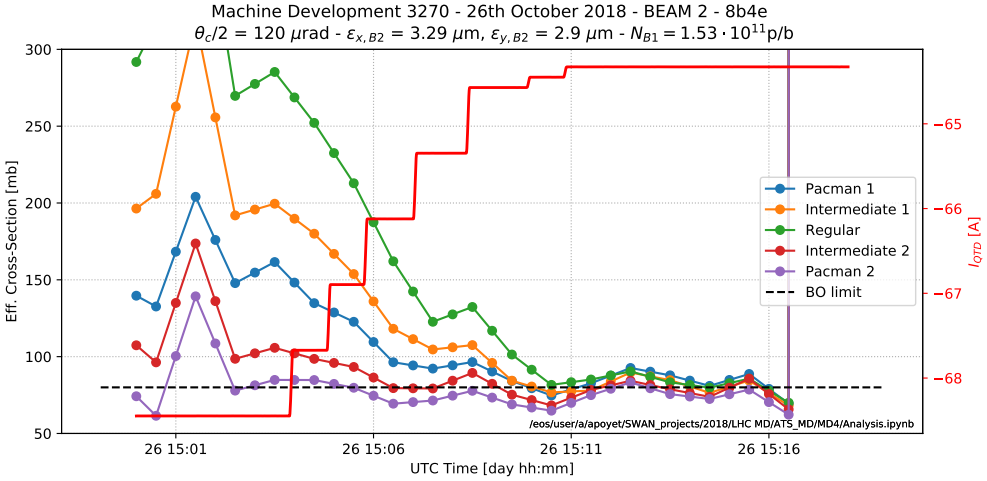

Beam 2

Figure 23: Tune scan in collision at $\beta^* = 65$ cm, with a half-crossing angle of $120\,\mu$rad in IR1 and IR5 ($9.3\,\sigma$ for a beam emittance of $\gamma\epsilon = 3.0\,\mu$m), and $N \sim 1.5 \times 10^{11}$ p/b (8b4e bunch trains): effective cross-section (i.e. loss rate normalised to luminosity) for a few bunches selected in Beam 1 (top) and Beam 2 (bottom), namely at the two extremities of the BCMS train (pacmam 1 and pacman 2), at half-distance between the extremities and the center of the train (intermediate 1 and intermediate 2), and at the center (regular). Each of the five steps of QTD current on the right scale corresponds to a tune shift of $\Delta Q_x = \Delta Q_y = 0.001$ along the diagonal (w.r.t. the nominal collision tune .31/.32). The last two small steps correspond to an horizontal tune shift of $\Delta Q_x = 0.001$ at constant vertical tune.

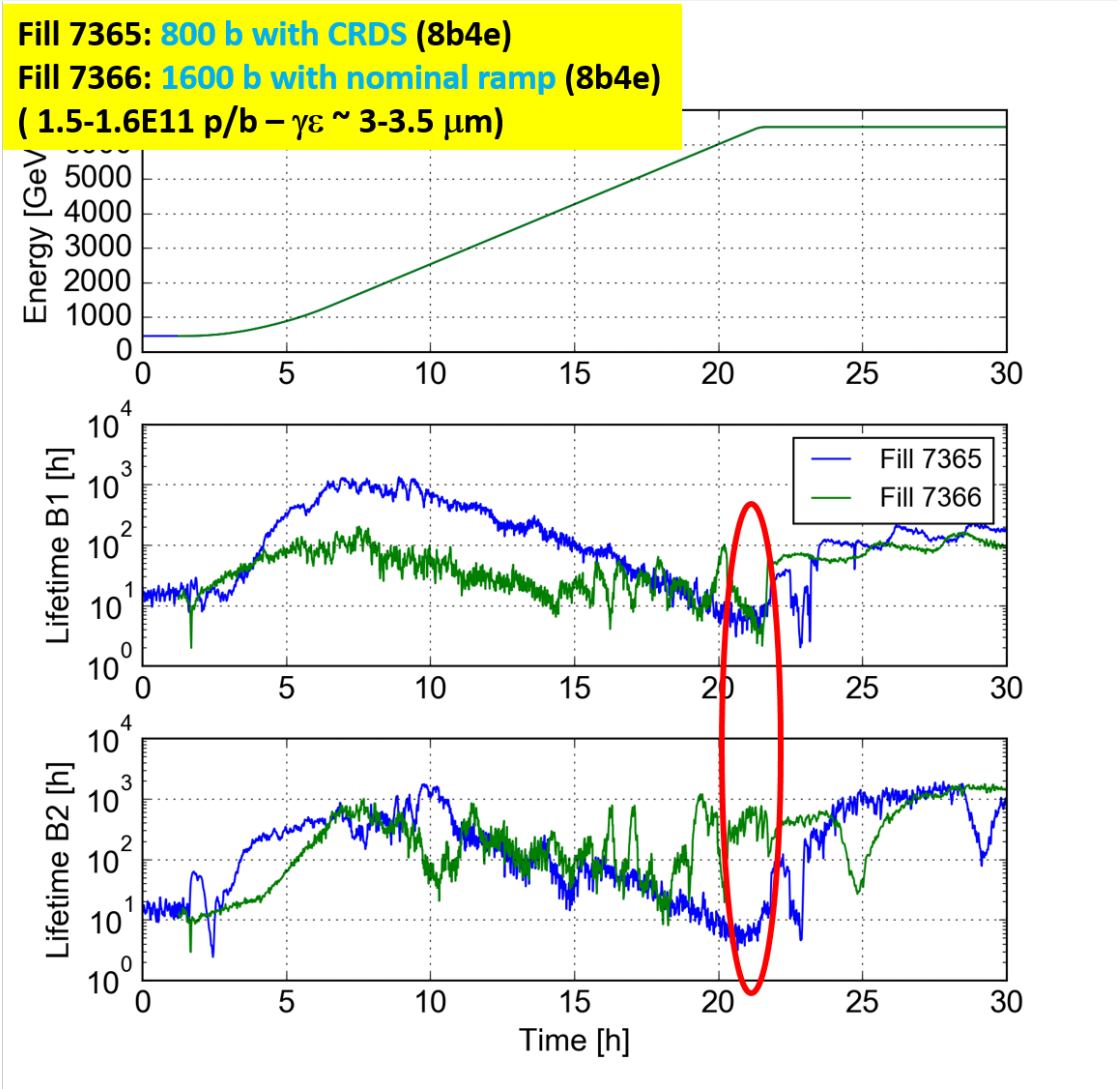

Figure 24: Beam lifetime measured in MD4 (8b4e bunch trains) for the CRDS (fill 7365 with $\sim$ 800 bunches) compared the nominal ramp (fill 7366 with $\sim$ 1600 bunches).

3.6 Instability observations

This section gives the exhaustive list of instabilities which were observed at a few occasions with set-up and unsafe beams in MD2, MD3 and MD4. Only the non-colliding bunches were affected in the case of MD sessions with bunch trains (MD3 and MD4), except for special tests to study in detail the collapsing beam process and its possible variants (see Sub-Section 3.6.3). In this Section, σ will always refer to the measured beam sizes (i.e. corresponding to a beam emittance in the range of $\gamma\epsilon = 2$–2.5 μm).

3.6.1 Instabilities during ADJUST

During the two fills operated with the positive polarity of the octupoles from injection to first collisions, namely fill 6978 in MD2 (see Section 3.3), and fill 7171 in MD3 (see Section 3.4), instabilities were observed during ADJUST (see Fig. 25). In the first one, the instability appeared during the search for the collision point in ALICE. Both bunches of each beam were affected by this instability in the horizontal plane. At the moment of the onset of the instability, there was no measurable luminosity at IP2. On the other hand, based on the luminosity published by ATLAS and CMS, the full transverse offsets between the beams were approximately 1.8 and 1.4 σ at IP1 and IP5, respectively.
In fill 7171, only the single non-colliding bunch of Beam 1 was affected (put in bucket 1 with lower ADT gain, see filling pattern in Fig. 11), and the instability also occurred in the horizontal plane.

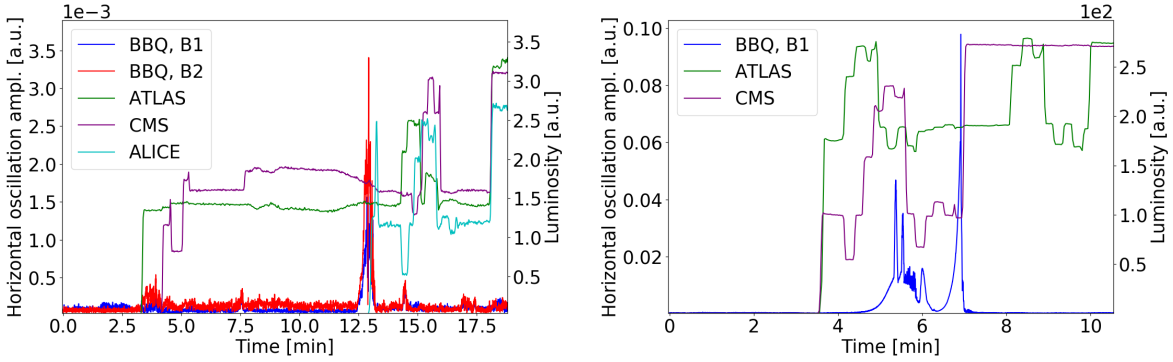

(a) Fill 6978 (MD2)

(b) Fill 7171 (MD3)

Figure 25: Horizontal oscillation amplitude and luminosity during ADJUST.

3.6.2 Instabilities during MO polarity swap

Few instabilities were observed during octupole polarity swaps. However, some of them affected bunches that had become unstable previously, thus deteriorating the quality of these bunches in a way that is not representative of normal running conditions. Figure 26 shows the very few cases of oscillation amplitudes measured during octupole polarity swaps performed in clean conditions only, i.e. without former instabilities.
In fill 6979 (set-up beams in MD2, see Section 3.3), the BBQ signal was found particularly noisy for both beams during the polarity swap from negative to positive [see Fig. 26(a)]. Nevertheless no increase of the signal was observed during the zero-crossing of the octupole current, and no

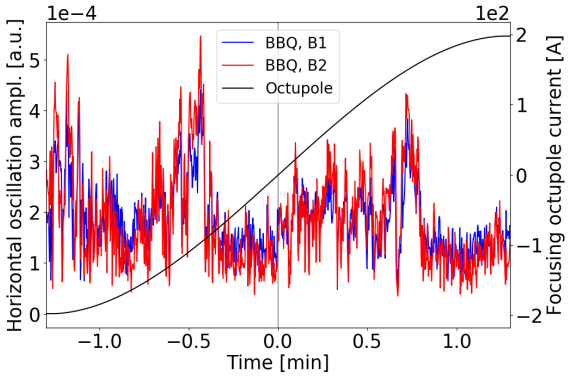

(a) Fill 6979 (MD2): first MO polarity swap

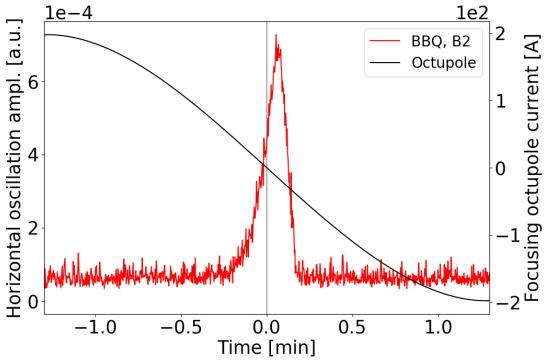

(b) Fill 7171 (MD3): first polarity swap

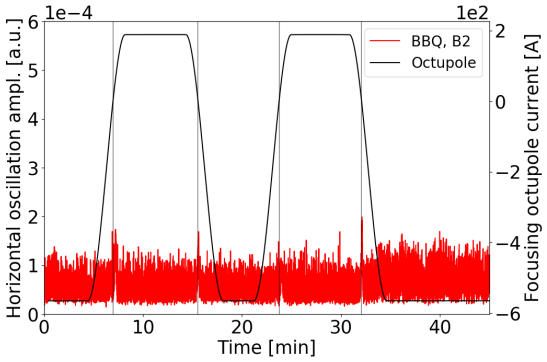

(c) Fill 7171: second to fifth polarity swap

Figure 26: Horizontal oscillation amplitude and octupole current measured during octupole polarity swaps. The times at which the octupole current crosses zero are marked with grey vertical lines.

coherent signal was picked up by the ADT activity monitor either.
On the other hand, a significant increase of the oscillation amplitude was measured in the middle of the first polarity swap from positive to negative during fill 7171 [see Fig. 26(b) for the non-colliding bunch of Beam 2, which was not found unstable earlier]. An increase of the amplitude correlated with the zero-crossing of the octupole current was also measured in the consecutive polarity swaps, yet with reduced amplitude [see Fig. 26(c)]. The onset of the rise of the oscillation amplitude during the first swap corresponds to an octupole current of $+50$ A, compatible with the estimated instability threshold calculated with DELPHI. The peak of the oscillation amplitude, which indicates the onset of a stabilization mechanism, is at -15 A. In all these cases no impact on the transverse emittance and beam intensity could be measured. The coherent signal was also not picked up by the ADT activity monitor, suggesting that it remained of low amplitude.

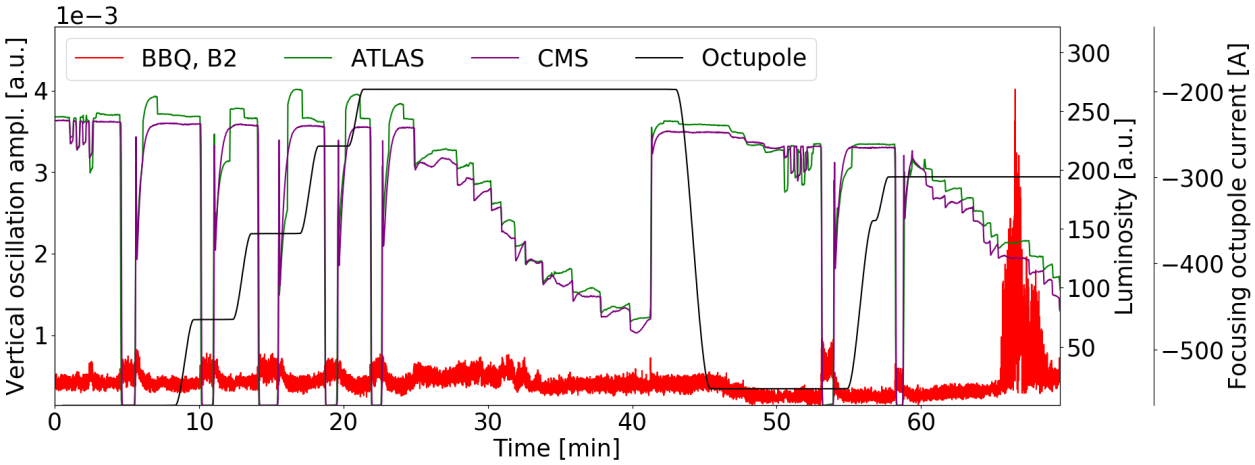

Figure 27: Vertical beam oscillation amplitude measured by the BBQ and luminosity measurements, for various MO currents, during synchronous separation scans at IP1 and IP5 at the end of fill 7171 (MD3). The beams are composed of an isolated non-colliding bunch followed by a train of 12b and a BCMS train colliding at IP1 and IP5, with no collision at IP2 and IP8 for none of the bunches, and no BBLR interaction between the 3 parts of the filling scheme (see Sub-Section 3.4.1). The half crossing angle between the beams was set to 120 μrad in IR1 and IR5.

3.6.3 Collapsing beam process and coherent instabilities

Slow versus fast synchronous separation scans at IP1 and IP5

At the end of fill 7171, a bit more than an hour was dedicated to the study of the beam stability with offset beams. The results of those tests are summarized in Fig. 27. The offset between the two beams was varied simultaneously at IP1 and IP5, perpendicularly to the crossing plane in each of these two IPs, using the *lumi scan knobs* to separate the beams up to a full separation of approximately 8σ, and then back to head-on collision.
The fast scans, i.e. when the separation is varied as fast as the power converters allow, are characterized by a sharp reduction of the luminosity followed by a return at the original values. These fast scans were performed with different powering of the arc octupoles, in a range of current between -550 A and -200 A (negative polarity). No instabilities were observed in any of those scans, neither from the BBQ signal, nor from the ADT activity monitor. No degradation of the transverse emittance and intensity could be measured either.
Then, two separation scans were performed in steps of approximately 0.1σ, with a steady phase of 1 minute at each step (so-called slow scan). The first slow scan (from minute 25 to 40 in Fig. 27) was performed with -200 A in the octupoles, and no instabilities were observed. During the second scan (minute 60 to 70 in Fig. 27), the MO current was set -300 A, and an instability was observed for a full separation of 1.6σ at IP1 and IP5. The measurement of single bunch oscillation amplitude shows that only a fraction of the bunches became unstable (Fig. 28).
This second slow scan was performed following a fast scan in exactly the same configuration (-300 A in the octupoles), demonstrating that the instability observed in the slow separation scan can actually be mitigated by a sufficiently fast collapse of the separation bumps.
The presence of instabilities during the slow scan at -300 A, as opposed to the same scan but with an octupole current of -200 A, can be understood as an impact of the compensation of the BBLR

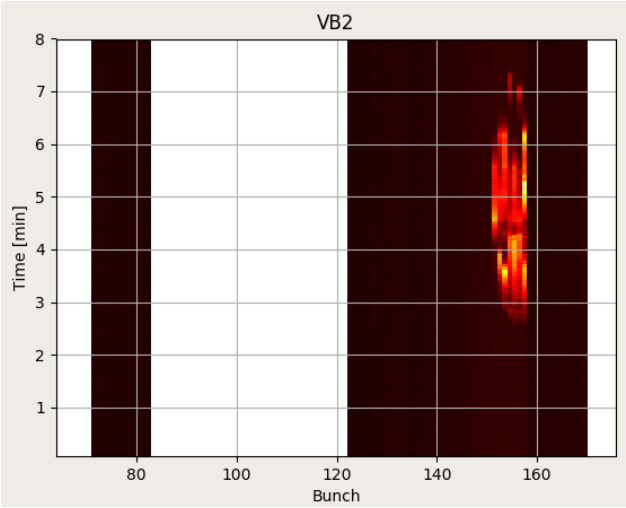

Figure 28: ADT activity monitor data during the instability observed in fill 7171 (MD3) during the second slow separation scan (see the last 10 minutes in Fig. 27).

induced tune spread by the lattice octupoles. These two contributions to the tune spread were compared quantitatively in [11], showing that PACMAN bunches were expected to be more critical than nominal bunches at -300 A, which is consistent with the single bunch oscillation measurements (Fig. 28). It remains however unclear why only an intermediate set of PACMAN bunches became unstable, i.e. on one side of the train only whereas bunches on each side experience a similar set of BBLR interactions. It is also unclear why this instability affected Beam 2 only.

Synchronous versus asynchronous or single plane separation scans at IP1 and IP5

During fill 7174, several tests were conducted to confirm that collapsing the separation bumps in one IP at a time, or in the same plane in both IPs, can be beneficial for the beam stability [14]. The machine was setup in the same configuration as the last separation scan in fill 7171, in particular with the MO current set to -300 A, such that the results can be compared directly.
The first two slow separation scans were performed maintaining the other IP separated at 8σ (minute 0 to 32 in Fig. 29). The separation was introduced with the *lumi scan knobs* in the plane perpendicular to the crossing plane in each IP. The BBQ signal was again quite noisy, but with no clear sign of any instabilities. No coherent signal was observed with the ADT activity monitor either. Another slow separation scan was performed simultaneously at IP1 and IP5, using exclusively the *lumi scan knobs* in the horizontal plane for both IPs (minutes 32 to 45). No instabilities were observed either. Finally a slow scan in the same conditions as for fill 7171 was performed (i.e. varying the *lumi scan knobs* in the plane perpendicular to the crossing plane in both IPs simultaneously). The instability was found again at a separation of 1.6σ (spike at ~ 55 min. in Fig. 29), thus demonstrating its possible mitigation by an asynchronous collapse of the separation bumps, or by the usage of the separation bumps in the same plane for both IPs.

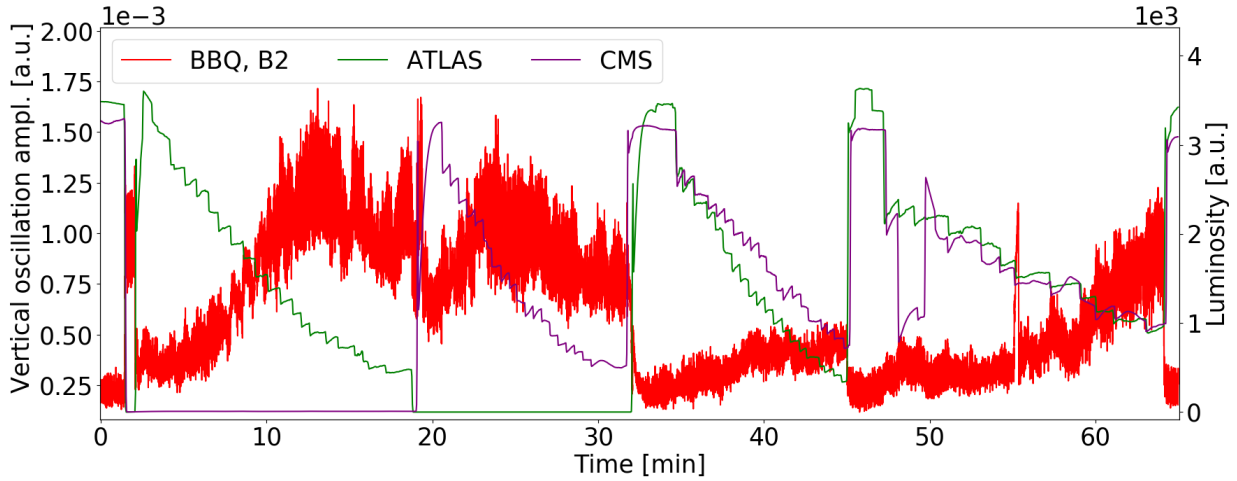

Figure 29: Vertical beam oscillation amplitude measured by the BBQ, and luminosity measurements during slow separation scans at IP1 and/or IP5: first at IP1 in the vertical plane (with the beams separated at IP5), then idem at IP5 in the horizontal plane, then simultaneously at IP1 and IP5 but in the horizontal plane for both IPs, and finally at both IPs in the plane perpendicular to the crossing plane. The measurement took place at the end of fill 7174 (MD3). The filling scheme is given in Fig. 11, the half crossing angle was set to 120 μrad in IR1 and IR5, and the MO current was -300 A (negative polarity).

4 Summary and outlook

A new LHC hypercycle, featuring a combined ramp and telescopic squeeze, was demonstrated in 2018, including an impressively fast intensity ramp up with up to 700 nominal bunches in MD3, and then the machine half-full with 8b4e bunch trains of high intensity in MD4. Such a machine configuration is mainly motivated by the mitigation of possible intensity limitations coming from the machine impedance for the high brightness beams which are foreseen in Run 3 and later on. The optics measurement and correction in the ramp can however become challenging, proportionally to the magnitude of the telescopic index which is targeted at flat-top energy (pushed up to $r_{\mathrm{Tele}} \sim 3.1$ at the EoR for the present MD hypercycle). Otherwise an improvement of the onset for instability was clearly demonstrated, with the octupole threshold reduced by a factor of about 2 with respect to the nominal hypercycle. Such a machine configuration could even open the possibility to run the full hypercycle with the negative polarity of the octupoles, instead of a possibly tedious procedure for reversing the MO polarity with the beam colliding, in order to directly profit from the usual beam-beam related by-products of telescopic optics: namely an improvement of the crossing angle reach by about $1\,\sigma$ thanks to an efficient and in-phase minimization via the lattice octupoles (with negative polarity) of the b_4-like components induced by the long-range beam-beam interactions.

Acknowledgements

The authors are grateful to the LHC machine coordination and the LHC machine protection panel for its support of the program in 2018. A special thank goes to G. Arduini, E. Métral and Y. Pa-

paphilippou for their accurate and patient work of proofreading and commenting the draft version of this manuscript. S. Redaelli is also acknowledged for the valuable feedback he gave to the collimation-related part of the MD programme.

References

[1] S. Fartoukh, "Achromatic Telescopic Squeezing scheme and its Application to the LHC and its Luminosity Upgrade", *Phys. Rev. ST Accel. Beams , Vol. 16, 111002*, 2013.

[2] H. Damerau *et al.*, "RF manipulations for higher beam brightness LHC-type beams", CERN-ACC-2013-0210.

[3] H. Damerau *et al.*, "LIU: Exploring alternative ideas", In proceedings of the Review of LHC and Injector Upgrade Plans Workshop, https://indico.cern.ch/event/260492/, 2018.

[4] S. Fartoukh, Optics repository for the 2018 LHC Round optics MDs, /afs/cern.ch/eng/lhc/optics/runII/2018/MDroundoptics2018/, 2018.

[5] S. Fartoukh, "MD3270: Telescopic round optics with pilots", MD Procedure for MD1, https://asm.cern.ch/api/files/1421741, 2018.

[6] R. Bruce *et al.*, "Reaching record-low β^* at the CERN Large Hadron Collider using a novel scheme of collimator settings and optics", in *Nuclear Instruments and Methods Section A, Vol. 848, pp. 19-30*, 2017.

[7] A. García-Tabarés Valdivieso and R. Tomás, "Optics-measurement-based beam position monitor calibrations in the LHC insertion regions", *Phys. Rev. Accel. Beams, Vol. 23, 042801*, 2020.

[8] A. Wegscheider, *et al.*, "Analytical N beam position monitor method", *Phys. Rev. Accel. Beam, Vol. 20, 111002*, 2017.

[9] S. Fartoukh, A. Mereghetti, M. Solfaroli, R. Tomas , "ATS activities in MD1-2018", presented at the CERN LHC Study Working Group (LSWG), 03/07/2018, https://indico.cern.ch/event/739768/.

[10] J. Scott Berg and F. Ruggiero, "Landau Damping with Two-Dimensional Betatron Tune Spread", CERN SL-AP-96-71 (AP), December 1996.

[11] X. Buffat, S. Fartoukh, "Instabilities with high tele index at the end of the ramp", presented at the 162nd ABP-HSI section meeting, 03/12/2018, https://indico.cern.ch/event/777486/.

[12] N. Fuster-Martinez, *et al.*, "Loss Maps validation YETS 2018 ", presented at the 230th LHC Collimation WG meeting 07/05/2018, https://indico.cern.ch/event/726453/.

[13] G. Iadarola, *et al.*, "Beam-induced heat loads on the LHC arc beam screens with different beam and machine configurations: experiments and comparison against simulations", CERN-ACC-NOTE-2019-0057, 2019.

[14] X. Buffat, *et al.*, "Strategy for Landau damping of head-tail instabilities at top energy in the HL-LHC", CERN-ACC Note in preparation,2020.

A TCT Centre Functions

This appendix shows the TCT center functions deployed in MD3270, compared to those used operationally. The plots show only the TCT center functions for the combined ramp and tele-squeeze. A selection of BPM readouts taken in MD fills with pilots and nominal bunches are shown as well, for comparison.

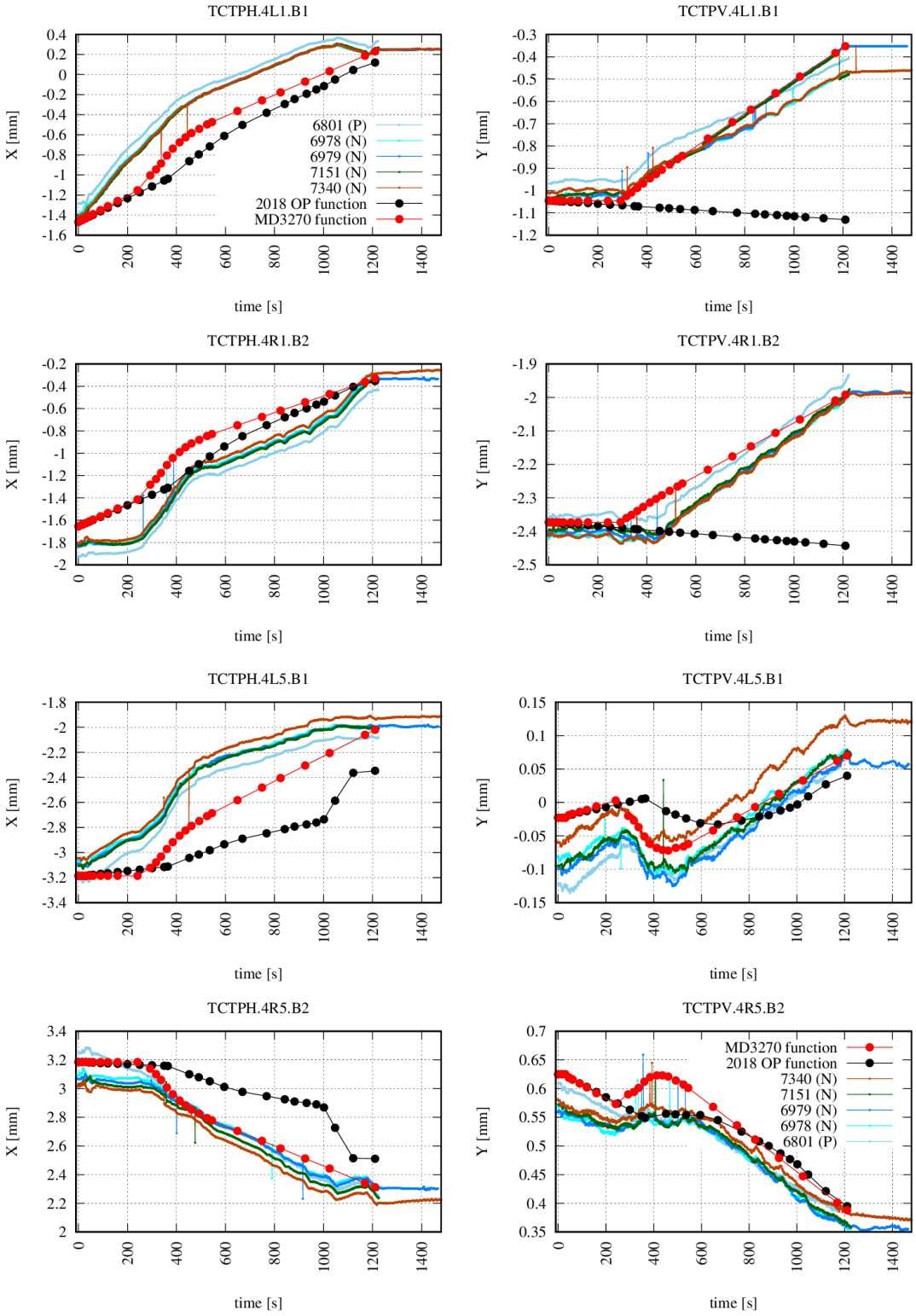

Figure 30: IR1 (top) and IR5 (bottom) TCT center functions deployed in MD3270 compared to those used operationally. A selection of BPM readouts taken in MD fills with pilots and nominal bunches are shown as well: the (P) label corresponds to a fill with pilot bunches only, whereas the (N) label refers to the fills where at least one nominal bunch was circulating in the machine.

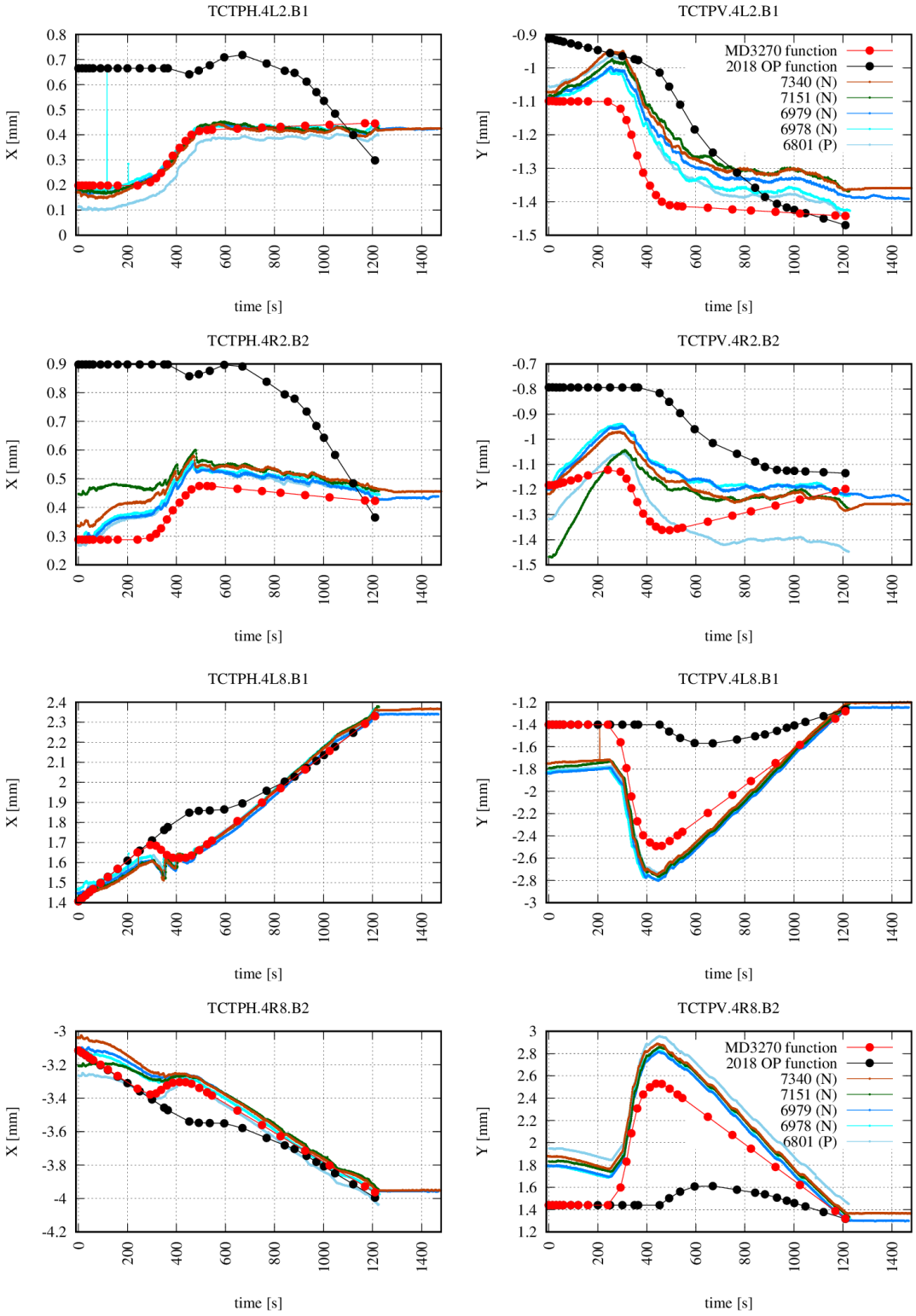

Figure 31: IR2 (top) and IR8 (bottom) TCT center functions deployed in MD3270 compared to those used operationally. A selection of BPM readouts taken in MD fills with pilots and nominal bunches are shown as well: the (P) label corresponds to a fill with pilot bunches only, whereas the (N) label refer to the fills where at least one nominal bunch was circulating in the machine.

B Collection of Reference Loss Maps

This appendix shows the qualification loss maps taken in fill 6979 (MD2) at flat-top energy (i.e. at the end of the ramp, before the tune change and the collapse of the separation bumps). The corresponding loss maps in collision are not shown, since patterns are essentially the same. This was also the case when the crossing angle in collision was decreased to 80 μrad (MD3 and MD4). In MD3 and MD4, off–momentum loss maps were taken as well, but are not shown here.
Qualification loss maps in MD4 were taken with the un–corrected B1 TCDQ functions (see section 2.2). They are very similar to those shown, apart from an increase by < 50 % at the TCDQ BLMs.
In MD2, loss maps where taken "on the fly" also during the ramp, i.e. at $\sim$2.7 TeV and 4.9 TeV, to make sure that the β–beating measured during the optics commissioning was tolerable in terms of performance of the collimation system, as it was expected. Since these loss maps did not show any noticeable pattern, they are also not shown.

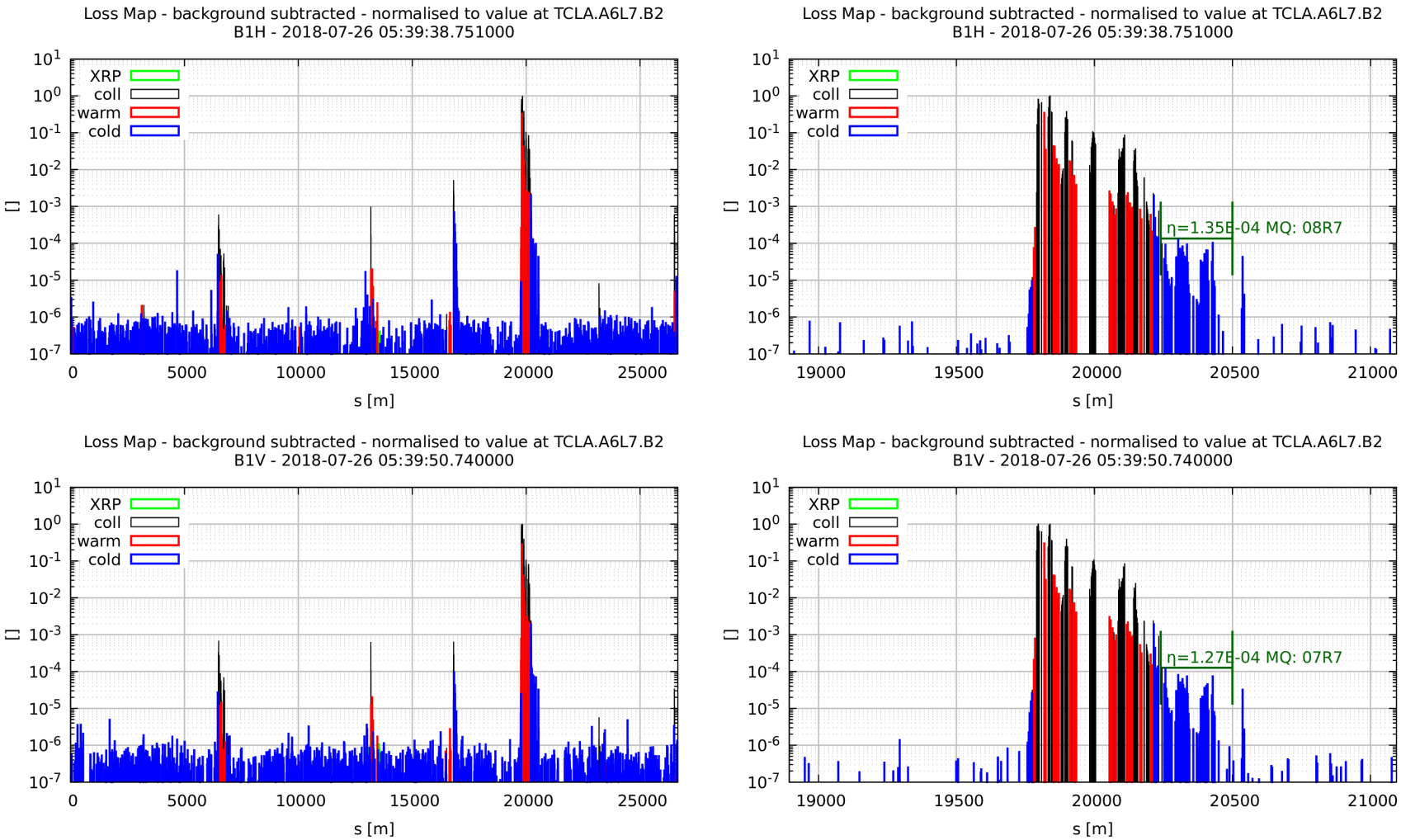

Figure 32: B1H (upper frames) and B1V (lower frames) loss maps at flat-top energy taken in fill 6979 during MD2.

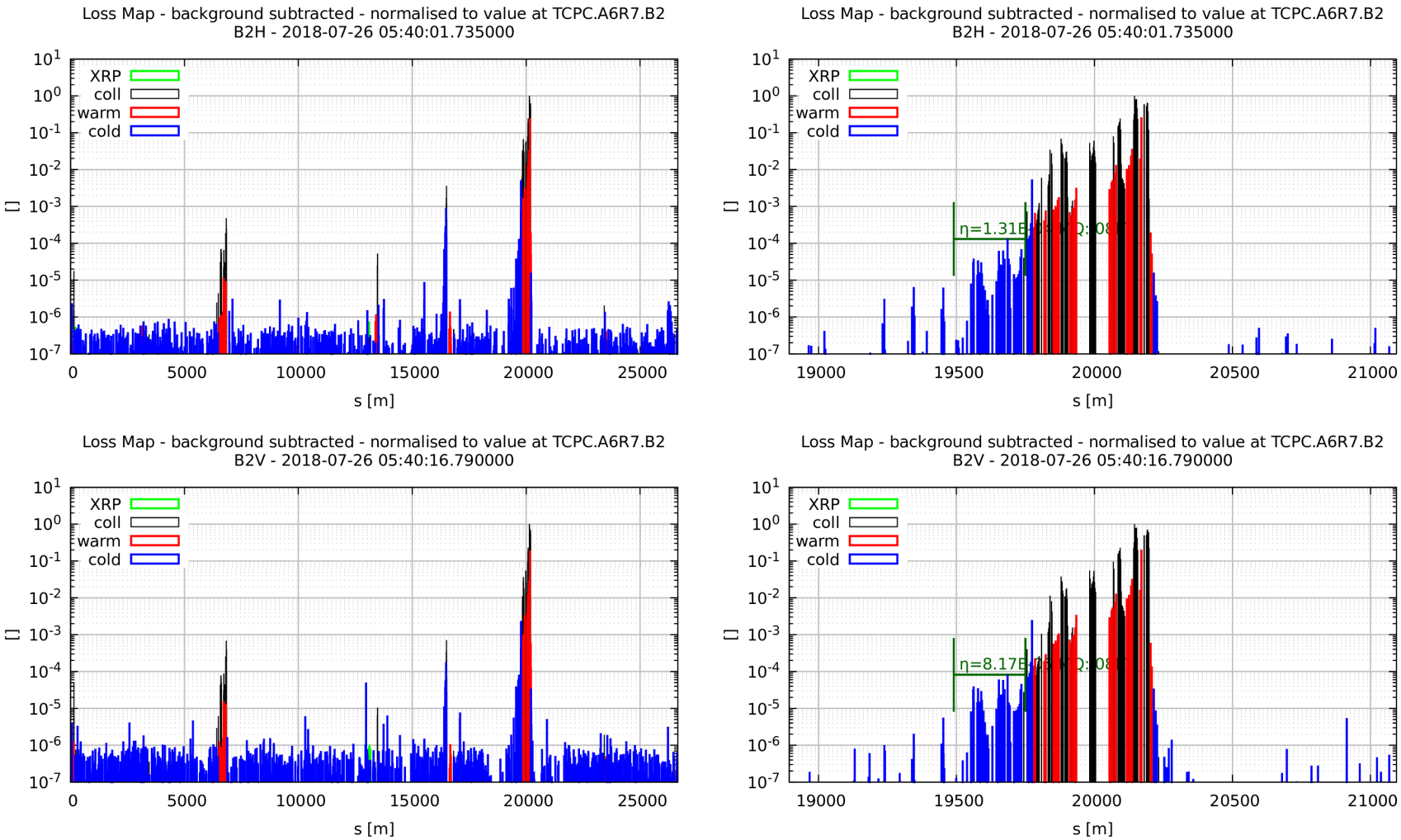

Figure 33: B2H (upper frames) and B2V (lower frames) loss maps at flat-top energy taken in fill 6979 during MD2.